



NRL/MR/5708--15-9629

Parametric Models of NIR Transmission and Reflectivity Spectra for Dyed Fabrics

D. AIKEN
S. RAMSEY
T. MAYO

*Signature Technology Office
Tactical Electronic Warfare Division*

S.G. LAMBRAKOS

*Center for Computational Materials Science
Materials Science and Technology Division*

J. PEAK

*Signature Technology Office
Tactical Electronic Warfare Division*

July 29, 2015

REPORT DOCUMENTATION PAGE			<i>Form Approved</i> <i>OMB No. 0704-0188</i>		
Public reporting burden for this collection of information is estimated to average 1 hour per response, including the time for reviewing instructions, searching existing data sources, gathering and maintaining the data needed, and completing and reviewing this collection of information. Send comments regarding this burden estimate or any other aspect of this collection of information, including suggestions for reducing this burden to Department of Defense, Washington Headquarters Services, Directorate for Information Operations and Reports (0704-0188), 1215 Jefferson Davis Highway, Suite 1204, Arlington, VA 22202-4302. Respondents should be aware that notwithstanding any other provision of law, no person shall be subject to any penalty for failing to comply with a collection of information if it does not display a currently valid OMB control number. <i>PLEASE DO NOT RETURN YOUR FORM TO THE ABOVE ADDRESS.</i>					
1. REPORT DATE (DD-MM-YYYY) 29-07-2015		2. REPORT TYPE Memorandum		3. DATES COVERED (From - To) June 2014 – May 2015	
4. TITLE AND SUBTITLE Parametric Models of NIR Transmission and Reflectivity Spectra for Dyed Fabrics			5a. CONTRACT NUMBER		
			5b. GRANT NUMBER		
			5c. PROGRAM ELEMENT NUMBER		
6. AUTHOR(S) D. Aiken, S. Ramsey, T. Mayo, S.G. Lambrakos, and J. Peak			5d. PROJECT NUMBER		
			5e. TASK NUMBER		
			5f. WORK UNIT NUMBER		
7. PERFORMING ORGANIZATION NAME(S) AND ADDRESS(ES) Naval Research Laboratory, Code 5708 Tactical Electronic Warfare Division Signature Technology Office 4555 Overlook Avenue, SW Washington, DC 20375-5320			8. PERFORMING ORGANIZATION REPORT NUMBER NRL/MR/5708--15-9629		
9. SPONSORING / MONITORING AGENCY NAME(S) AND ADDRESS(ES) Program Management Office U.S. Army Natick Soldier Research Special Operations Forces Development and Engineering Center Survival Support & Equipment Systems 15 Kansas Street Natick, MA 01760-5000			10. SPONSOR / MONITOR'S ACRONYM(S) PM-SOF SSES		
			11. SPONSOR / MONITOR'S REPORT NUMBER(S)		
12. DISTRIBUTION / AVAILABILITY STATEMENT Approved for public release; distribution is unlimited.					
13. SUPPLEMENTARY NOTES					
14. ABSTRACT This study examines parametric modeling of near-infrared (NIR) transmission and reflectivity spectra for dyed fabrics, which provides for both their inverse and direct modeling. The dyes considered for prototype analysis are triarylamine, tetraaryldiamine, transition metal dithiolene, and indolium iodide. The fabrics considered are camouflage textiles characterized by color variations. The results of this study provide validation of the constructed parametric models, within reasonable error tolerances for practical applications, including NIR spectral characteristics in camouflage textiles, for purposes of simulating NIR spectra corresponding to various dye concentrations in host fabrics, as well as potentially to mixtures of dyes.					
15. SUBJECT TERMS Parametric Modeling Absorption coefficient Inverse/direct analysis NIR/SWIR absorbing dyes Dielectric function Reflection/transmission					
16. SECURITY CLASSIFICATION OF:			17. LIMITATION OF ABSTRACT	18. NUMBER OF PAGES	19a. NAME OF RESPONSIBLE PERSON Daniel Aiken
a. REPORT Unclassified Unlimited	b. ABSTRACT Unclassified Unlimited	c. THIS PAGE Unclassified Unlimited			Unclassified Unlimited

Contents

Introduction.....	1
Parametric Models of NIR Spectra for Dyed Fabrics.....	2
Case Study: Analyses of NIR Spectra for Dyed Fabrics.....	4
Conclusion.....	5
Acknowledgement.....	5
References.....	5

Parametric Models of NIR Transmission and Reflectivity Spectra for Dyed Fabrics

Introduction

Parametric models of NIR transmission and reflectivity spectra for dyed fabrics are presented, which provides for both their inverse and direct modeling [1]. The fabrics considered are camouflage textiles characterized by color variations. The dyes considered for prototype analysis are triarylamine (Dye 978), tetraaryldiamine (Dye 949), transition metal dithiolene (Dye 836) and indolium iodide (Dye 775) [2]. These dyes are within classes that are of interest to the U.S. Navy for the purpose of developing specific NIR spectral characteristics in camouflage textiles and other materials. The results of this study provide validation of the constructed parametric models, within reasonable error tolerances for practical applications, including NIR spectral characteristics in camouflage textiles, for purposes of simulating NIR spectra corresponding to various dye concentrations in host fabrics, as well as potentially to mixtures of dyes. Further, the results of this study demonstrate that absorption coefficients for dyes, which have been obtained previously by inverse analysis of transmission spectra for dyes in solution, can be validated as reasonable estimates of absorption coefficients for dyes in fabrics, which may be characterized as solid composite systems. Further, this study demonstrates proof of concept for parametric modeling of reflection from dyed fabrics by adopting a formalism similar to that of multicomponent analysis of spectra, which is typically for analysis of transmission through solutions containing varieties of solvents.

Parametric Models of NIR Spectra for Dyed Fabrics

Physically consistent parametric models provide a means for investigating the dielectric response characteristics of a given system that is characterized by a given material, or combination of materials, and geometry, in terms of both inverse and direct analysis [1]. For transmission through and reflection from a dyed fabric of finite and nonuniform thickness, whose material composition is heterogeneous, a general framework for parametric modeling of transmission and reflectivity spectra is given by

$$T_{f+d,M}(\lambda) = \exp \left[\sum_{j=1}^N C_{a,j} \alpha_{M,j}(\lambda) d \right] T_f(\lambda) \quad (1a)$$

$$T_{f+d,M}(\lambda) = \left[1 - \sum_{j=1}^N C_{a,j} \alpha_{M,j}(\lambda) d \right] T_f(\lambda) \quad (1b)$$

$$Z_T = \sum_{n=1}^N w_n \left(T_{f+d,M}(\lambda_n) - T_m(\lambda_n) \right)^2 \quad (2)$$

$$R_{f+d,M}(\lambda) = \exp \left[\sum_{j=1}^N A_{a,j} \alpha_{M,j}(\lambda) \right] R_f(\lambda) \quad (3a)$$

$$R_{f+d,M}(\lambda) = \left[1 - \sum_{j=1}^N A_{a,j} \alpha_{M,j}(\lambda) \right] R_f(\lambda) \quad (3b)$$

$$Z_R = \sum_{n=1}^N w_n \left(R_{f+d,M}(\lambda_n) - R_m(\lambda_n) \right)^2 \quad (4)$$

where d is the average thickness of the fabric layer, and α is the absorption coefficient. The formal procedure underlying inverse analysis based on Eqs.(1)-(4) entails adjustment of the absorption coefficients defined over the entire wavelength region, if assumed unknown, and the concentration coefficients C_a and A_a . This approach defines an optimization procedure where the transmission or reflectivity spanning the range of wavelengths is adopted as the quantity to be optimized. Constraint conditions are imposed on the transmission or reflectivity by minimizing the objective functions defined by Eqs. (2) and (4), respectively, where $T_m(\lambda_n)$ and $R_m(\lambda_n)$ are the measured or target transmission and reflectivity for wavelength λ_n . The quantities $w_n(n=1, \dots, N)$ are weight coefficients that specify relative levels of influence associated with constraint conditions $T_m(\lambda_n)$ and $R_m(\lambda_n)$.

The mathematical foundation of inverse analysis based on Eqs.(1)-(4) is that of least-squares parameter optimization [3, 4]. A significant aspect of least-squares parameter optimization is the choice of a sufficiently complete set of basis functions. This implies that all possible modes of a given process can be modeled parametrically by linear combinations of these functions. Accordingly, the parametric models defined by Eqs. (1a,b) and (3a,b) adopt absorption coefficients as basis functions. The general forms of Eqs. (1a,b) and (3a,b) are based on trend features following those of the Beer-Lambert law. Their parameterizations, however, are phenomenological in nature.

Direct modeling (or system simulation) based on Eqs.(1a,b) and (3a,b) provides a means for predicting the dielectric response characteristics of a layer of dyed fabric. For the case of a layer of dyed fabric, direct modeling assumes that material properties, e.g. absorption coefficients, have been estimated reasonably and that model parameters represent system response for the range of variation of quantities characterizing the system, e.g., dye concentration, as well as quantities or metrics associated with the dyeing process or with fabric characteristics.

Case Study: Analyses of NIR Spectra for Dyed Fabrics

In this section, prototype analyses of NIR transmission and reflectivity spectra for dyed fabrics are described. The fabrics considered are camouflage textiles characterized by color variations. The dyes considered for prototype analysis are triarylamine, tetraaryldiamine, transition metal dithiolene and indolium iodide [2]. For the spectra analyzed, our goal is to parametrically model the transmission and reflection characteristics of the dyes as a function of concentration.

First, we seek to parametrically model transmission characteristics of the dyes as a function of concentration. Shown in Figs. (1)-(4) are measured transmission spectra for dyed fabrics as a function of dye concentration. Accordingly, we define the quantity

$$T_{d,E}(\lambda, C_a) = \frac{T_{f+d,E}(\lambda, C_a)}{T_{f,E}(\lambda)} = C_o \frac{T_{f+d,E}(\lambda, C_a)}{\langle T_{f,E}(\lambda) \rangle} \quad (5)$$

where, because of small spectral variations for the untreated fabric associated with different colors (see Figs. (5) and (6)), we introduce the scaling parameter C_o , which represents small adjustments on the order of unity. This follows in that the transmission defined by Eq.(5) is based on background subtraction using an averaged transmission spectrum $\langle T_{f,E}(\lambda) \rangle$ for the untreated fabric, which is shown in Fig. (7). Next, adopting the parametric model Eq.(1a), and assuming background subtraction with a scale factor C_o , the modeled transmission component of the dyes as a function of concentration is given by

$$T_{d,M}(\lambda, \beta) = C_o \frac{T_{f+d,M}(\lambda, C_a)}{T_f(\lambda)} = C_o \exp[C_a \alpha_M(\lambda) d] = C_o \exp[-\beta \alpha_M(\lambda)] \quad (6)$$

where $\beta = C_a d$. The transmission defined by Eq.(6) assumes that the quantities C_a and d are averaged quantities in that the dyed fabrics do not have uniform thickness and are heterogeneous in composition. Accordingly, their combined influence is represented by a single adjustable parameter. Proceeding, values of the parameters C_o and β as a function of dye concentration are determined. Estimates of the absorption coefficients $\alpha_M(\lambda)$ for the dyes considered have been determined previously by inverse analysis of transmission spectra for these dyes in solution. For this analysis, we do not consider parameter optimization in the strict sense of objective function minimization, but rather a relaxed parameter adjustment with respect to qualitative agreement of measured and modeled spectra. It is important to note that a relaxed criterion for parameter optimization is consistent with the statistical nature of the measured spectra, which are for a nonuniform and irregular system. Shown in Figs. (8)-(11) are comparisons of experimental and modeled spectra, defined by Eqs. (5) and (6), respectively.

Next, we seek to parametrically model reflectivity characteristics of the dyes as a function of concentration. Shown in Figs. (12)-(15) are the reflectance spectra of untreated $R_{f,E}$ and dyed fabric $R_{f+d,E}$ as a function of dye concentration. Shown in Figs. (16)-(19) are scaled absorption coefficients as a function of dye concentration defined by

$$A_a \alpha_E(\lambda) = 1 - \frac{R_{f+d,E}(\lambda, A_a)}{R_{f,E}(\lambda)}, \quad (7)$$

where the phenomenological coefficient A_a is proportional to the density of dye molecules extending over a penetration depth of the fabric and inversely proportional to the level of scattering. The experimental quantity defined by Eq.(7) is modeled parametrically by the scaled absorption coefficient $C_a\alpha_M(\lambda)$. Shown in Figs. (20)-(23) are comparisons of measured and modeled absorption spectra, defined by Eq. (7) and $C_a\alpha_M(\lambda)$, respectively, where the absorption coefficients $\alpha_M(\lambda)$ have been determined previously by inverse analysis of transmission spectra for these dyes in solution. Again, for this analysis, we do not consider parameter optimization formally by means of objective function minimization, but rather relaxed parameter adjustment based on qualitative agreement of measured and modeled spectra. Shown in Fig. (24) are values of C_a as a function of dye concentration.

Conclusion

The fitting of modeled to experimental spectra shown in Figs. (8)-(11) and Figs. (20)-(23) for transmission and reflection, respectively, as well as the relatively good consistency of these fits, establishes proof of concept for constructing mappings from a process-parameter space, i.e., dye concentrations, to a model-parameter space, i.e., parameters C_o and β for transmission spectra and C_a for reflectivity spectra. This in turn establishes that the parametric models defined by Eqs. (1a,b) and (3a,b) can be adopted for prediction of dyed fabric transmission and reflection characteristics for process parameters that can be mapped into a physically consistent range of values for model parameters.

Acknowledgement

This work was supported by the Program Management Office, Special Operations Forces, Survival Support & Equipment Systems (PM-SOF SSES). We extend our appreciation to Drs. Miro Muzik and Oleg Ponomarev of Fabricolor Holding International, LLC, for their helpful insights in this effort.

References

1. A. Tarantola: Inverse Problem Theory and Methods for Model Parameter Estimation, SIAM, Philadelphia, PA, 2005.
2. Fabricolor Holding International Product List, Laser and Fluorecent dyes, UV and NIR dyes, security inks and other optically functional materials, Code FHI 97811, Code FHI 94931 and Code FHI 83642.
3. R.W. Farebrother, Linear Least Square Computations, Marcel Dekker, New York, 1988.
4. Y.B. Bard, Nonlinear Parameter Estimation, Academic Press, New York. 1974.

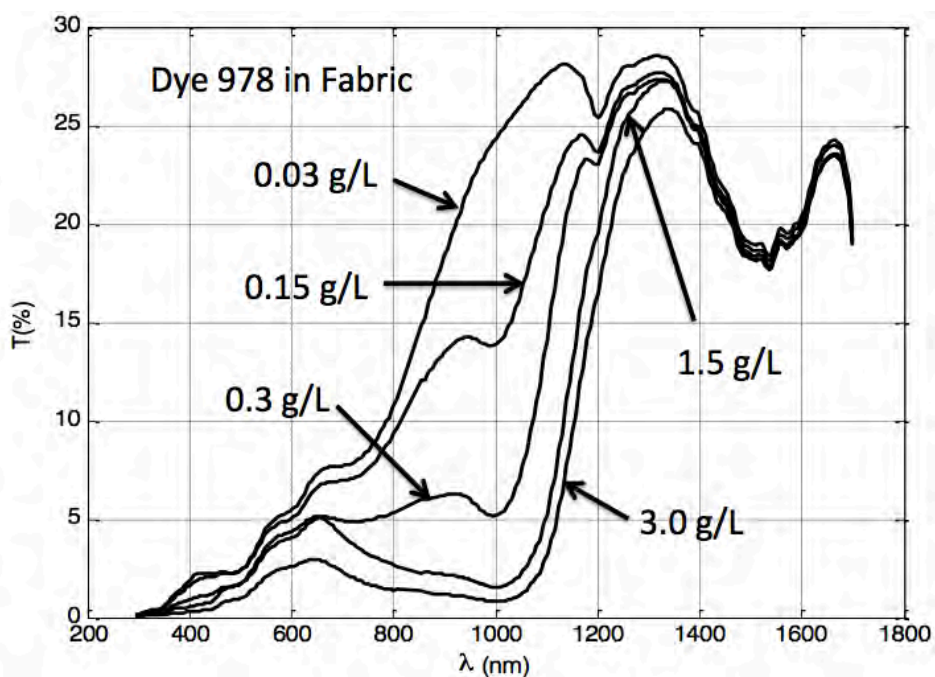


Figure 1. Experimentally measured transmission spectra for Triarylamine dye embedded in fabric as a function of dye concentration.

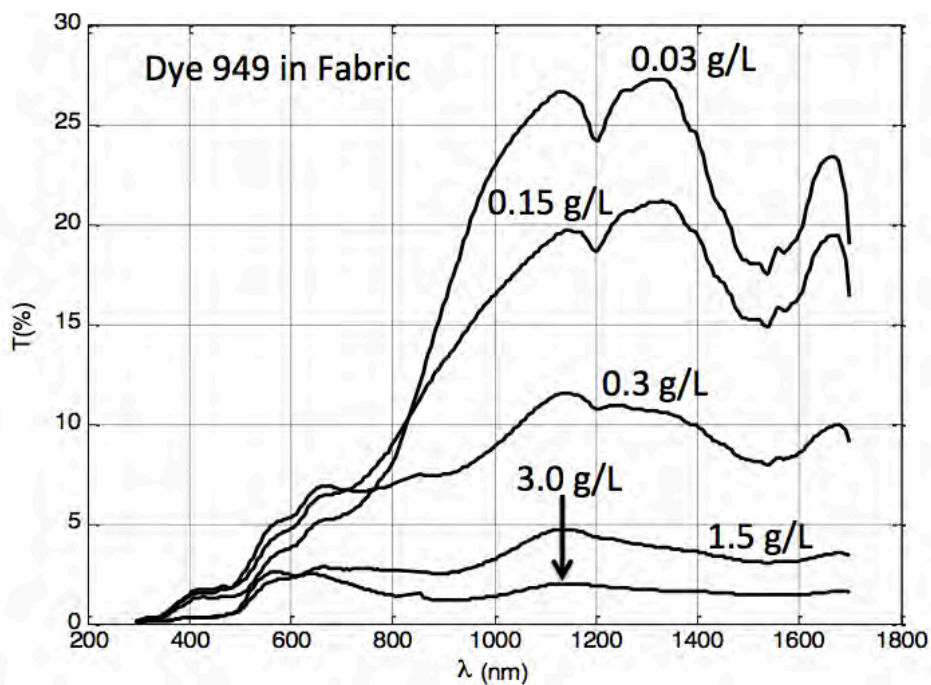


Figure 2. Experimentally measured transmission spectra for Tetraaryldiamine dye embedded in fabric as a function of dye concentration.

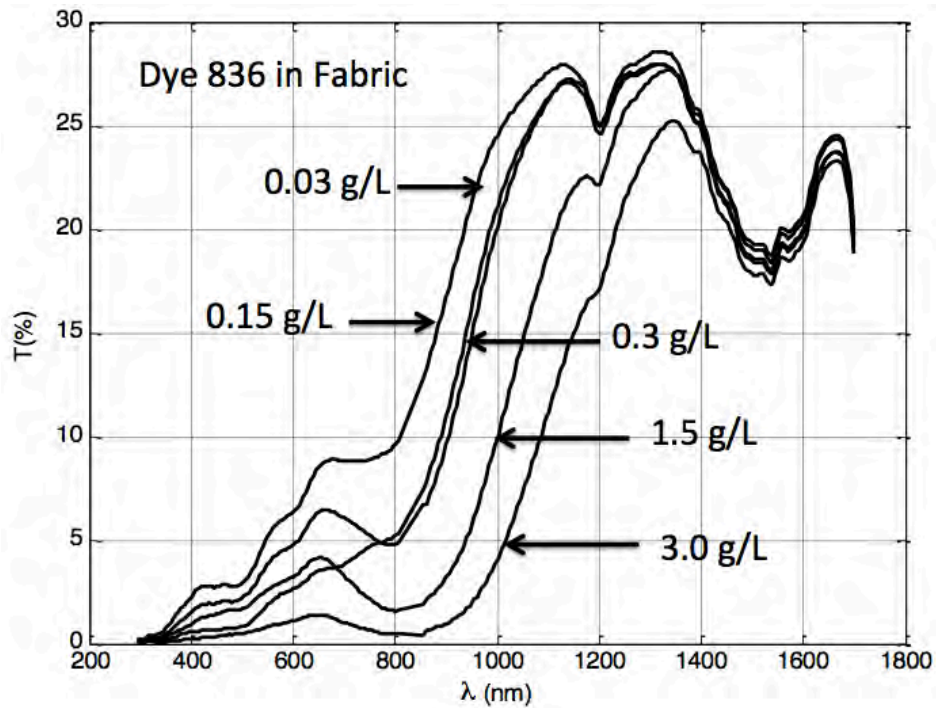


Figure 3. Experimentally measured transmission spectra for Transition Metal Dithiolene dye embedded in fabric as a function of dye concentration.

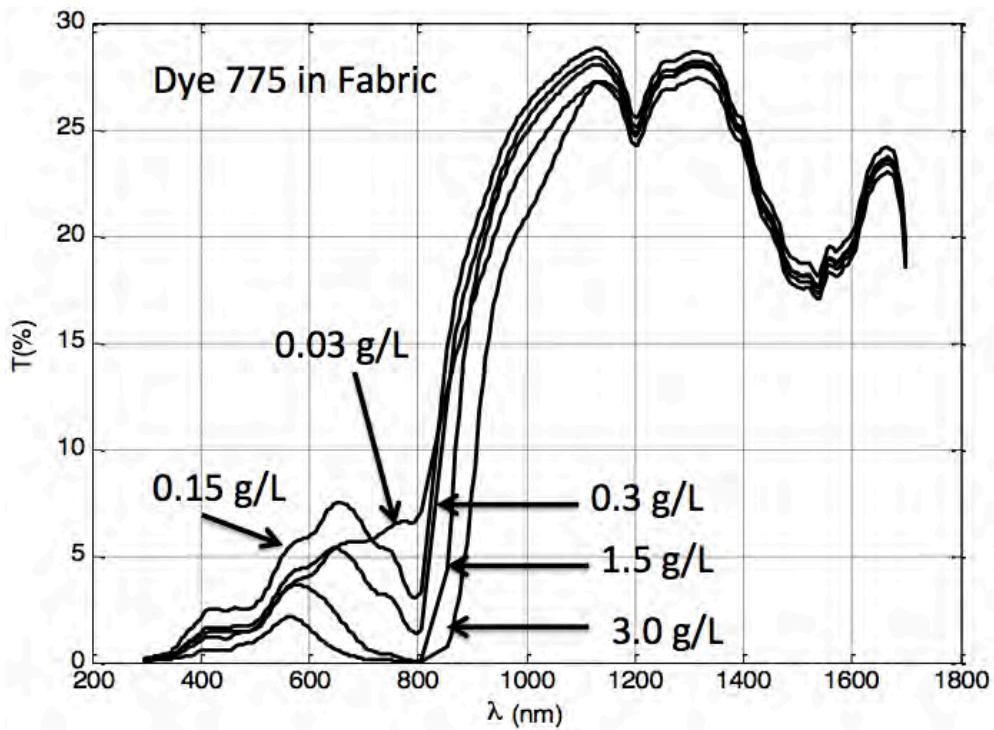


Figure 4. Experimentally measured transmission spectra for Indolium Iodide dye embedded in fabric as a function of dye concentration.

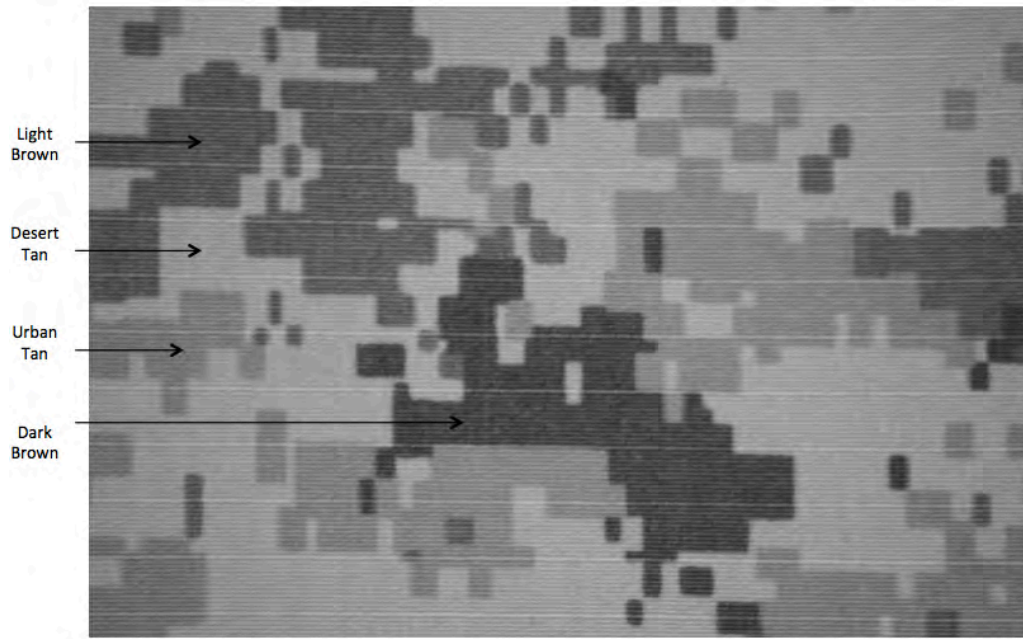


Figure 5. Different colors for fabric without dye.

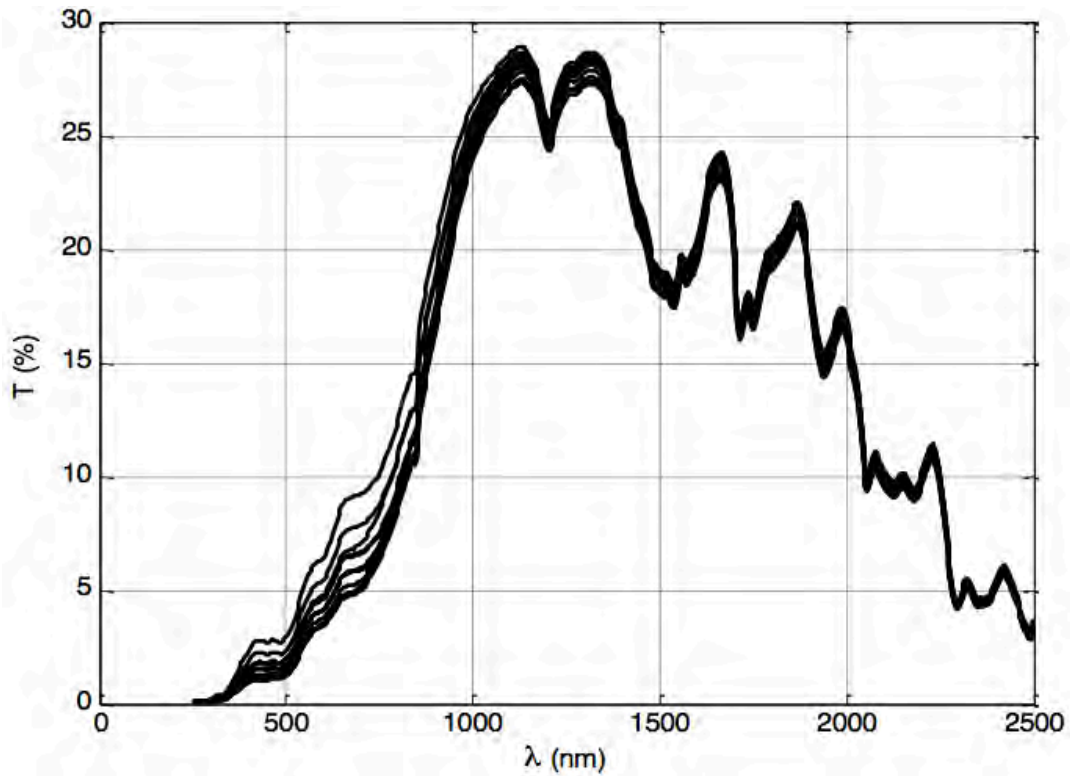


Figure 6. Experimentally measured transmission spectra showing small variations in the visible spectrum associated with the different colors shown in Fig. (5).

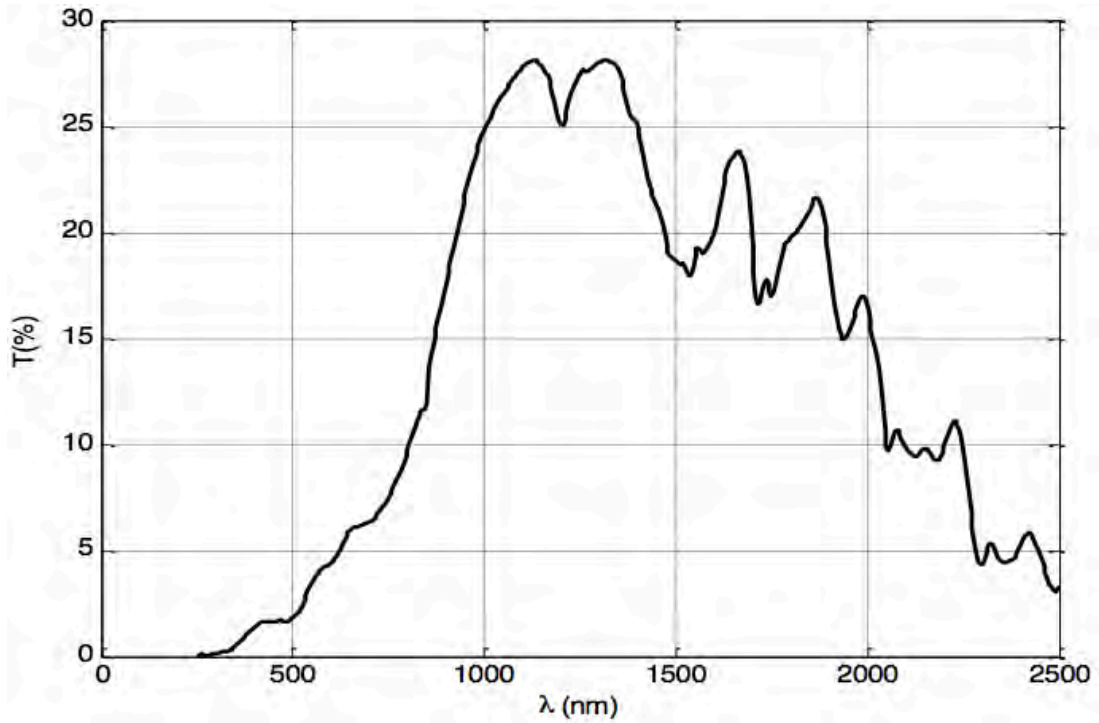


Figure 7. Averaged experimentally measured transmission spectrum of fabric without dye.

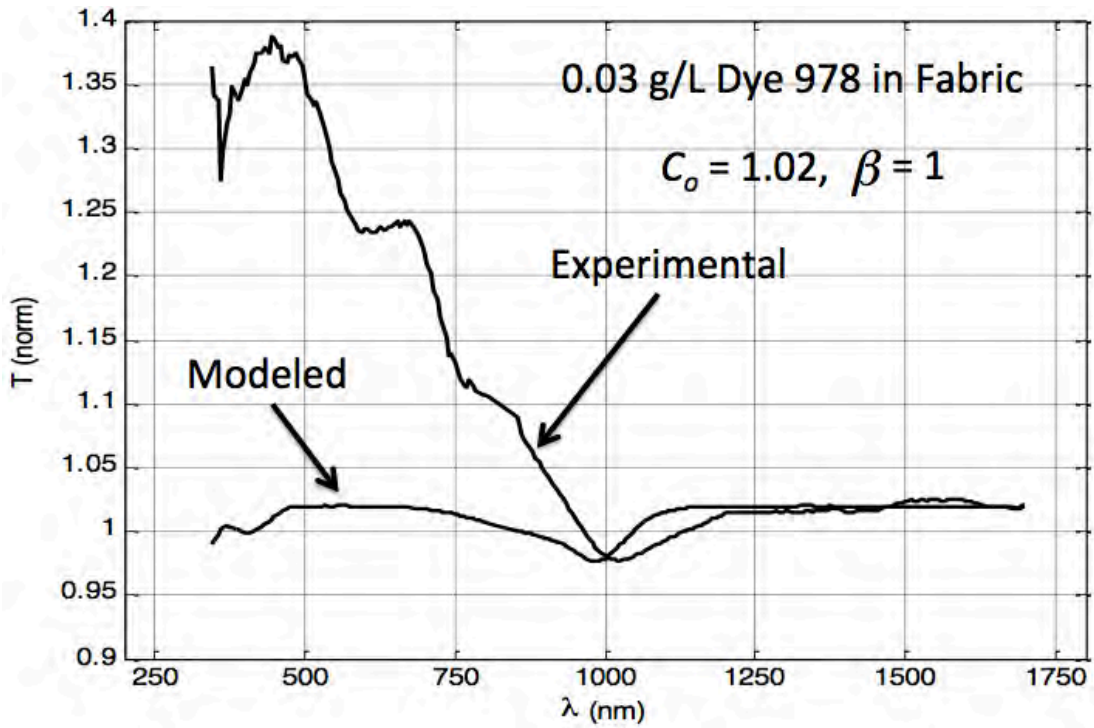


Figure 8a. Comparison of modeled and experimental transmission spectra defined by Eqs. (5) and (6), respectively.

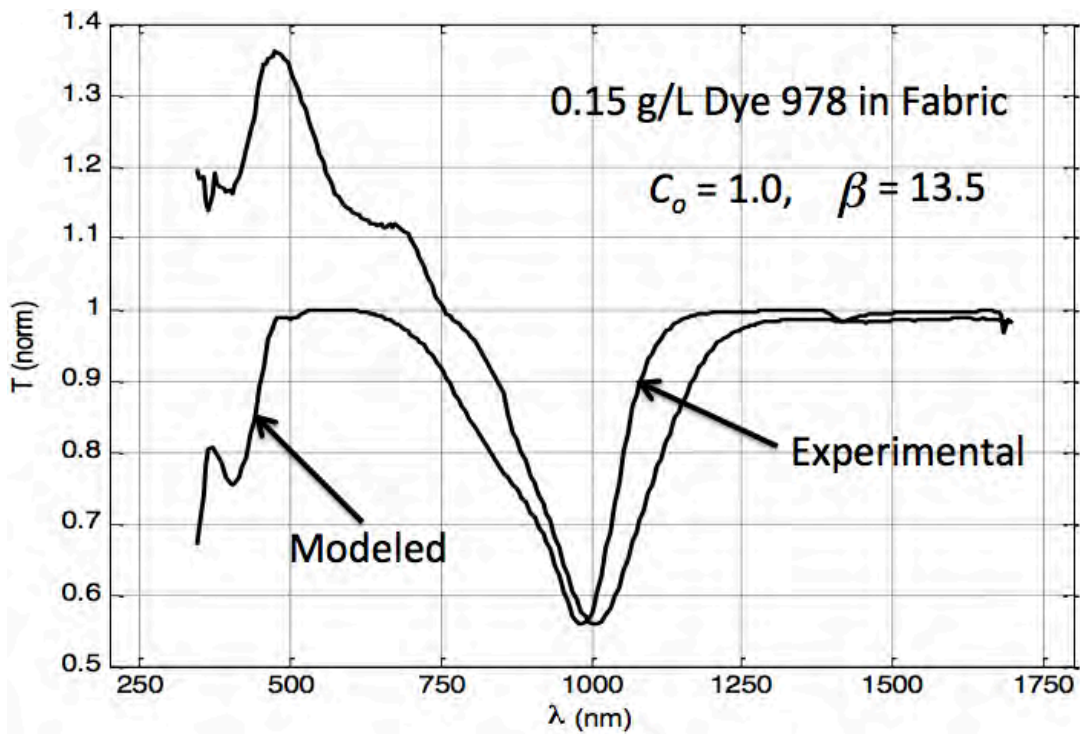


Figure 8b. Comparison of modeled and experimental transmission spectra defined by Eqs. (5) and (6), respectively.

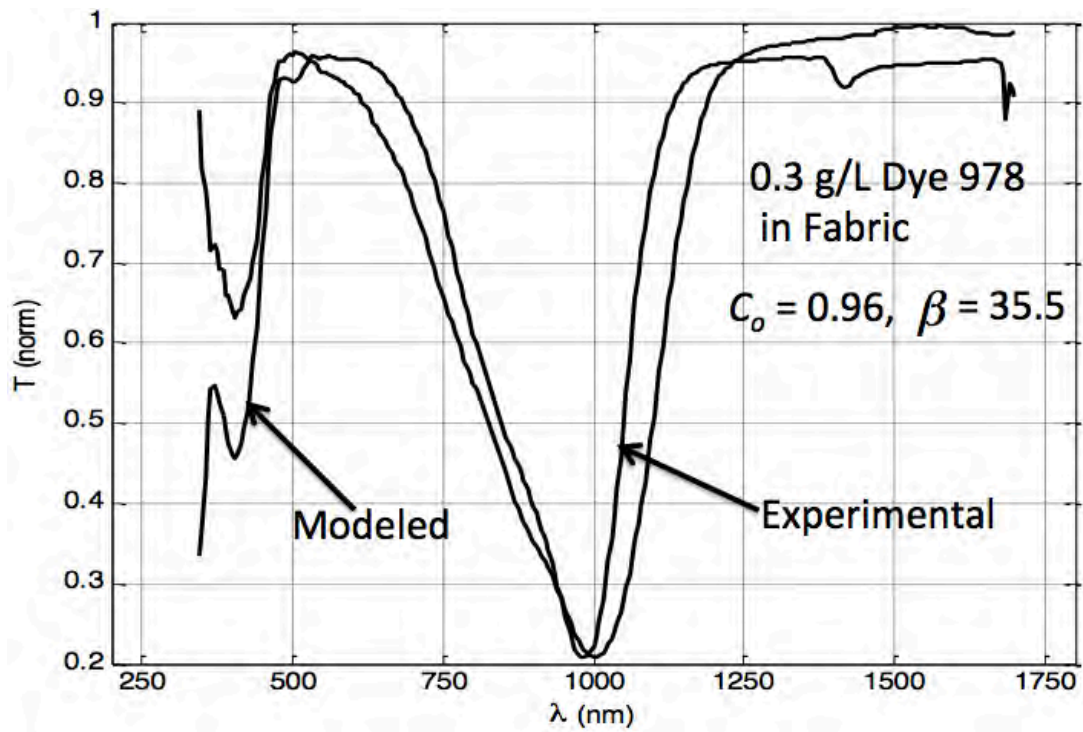


Figure 8c. Comparison of modeled and experimental transmission spectra defined by Eqs. (5) and (6), respectively.

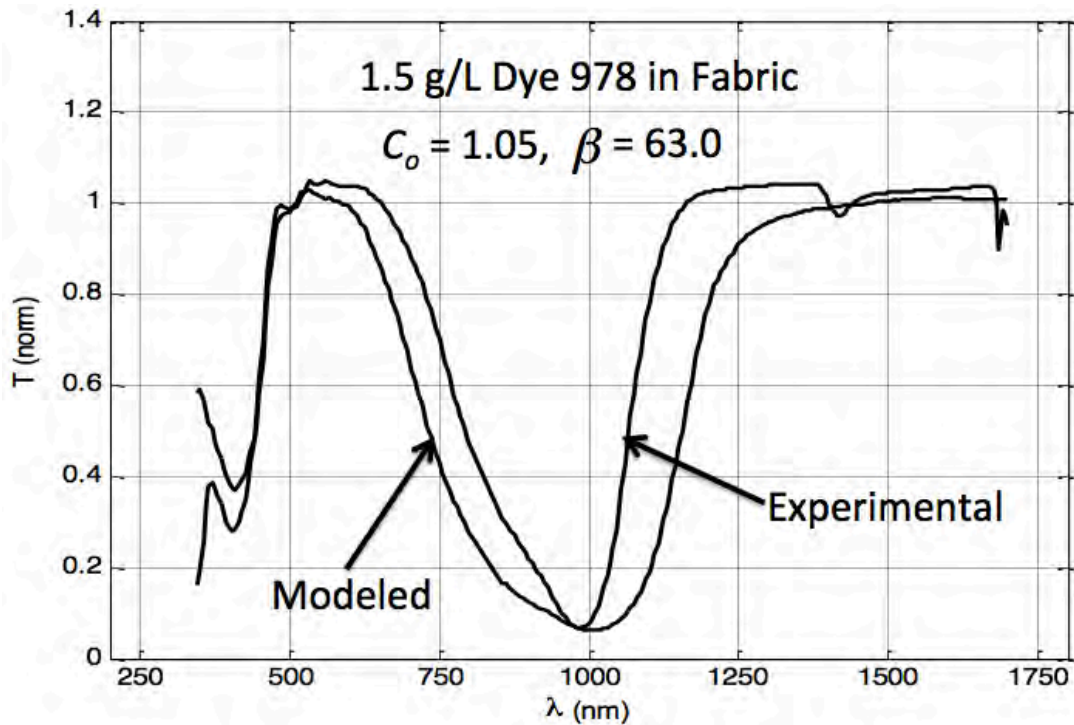


Figure 8d. Comparison of modeled and experimental transmission spectra defined by Eqs. (5) and (6), respectively.

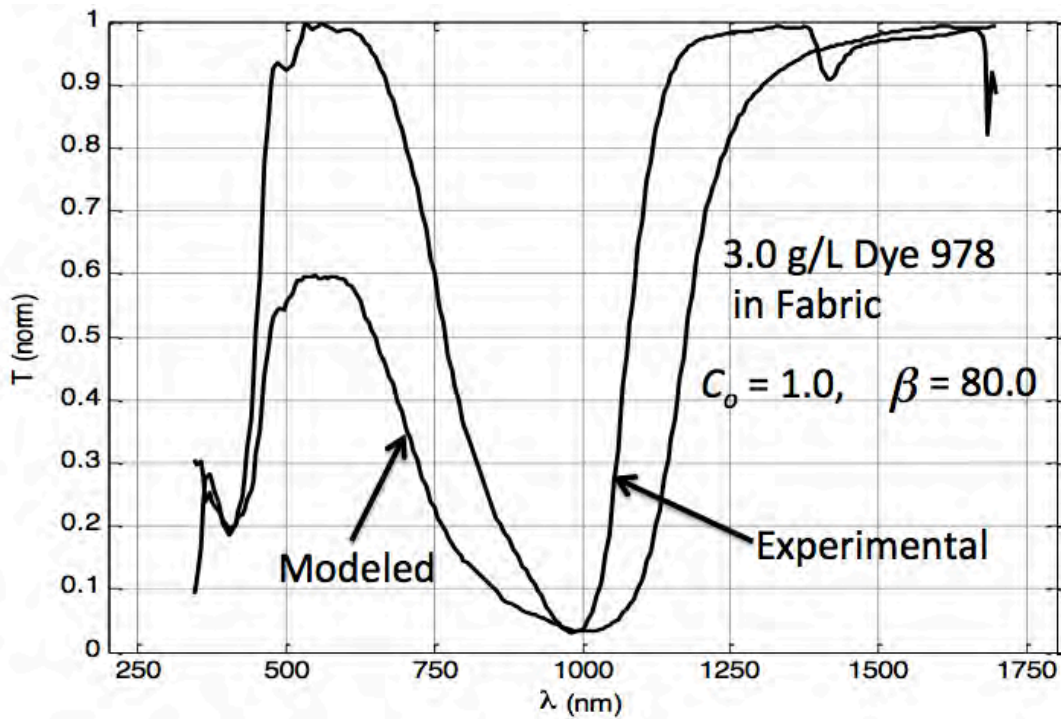


Figure 8e. Comparison of modeled and experimental transmission spectra defined by Eqs. (5) and (6), respectively.

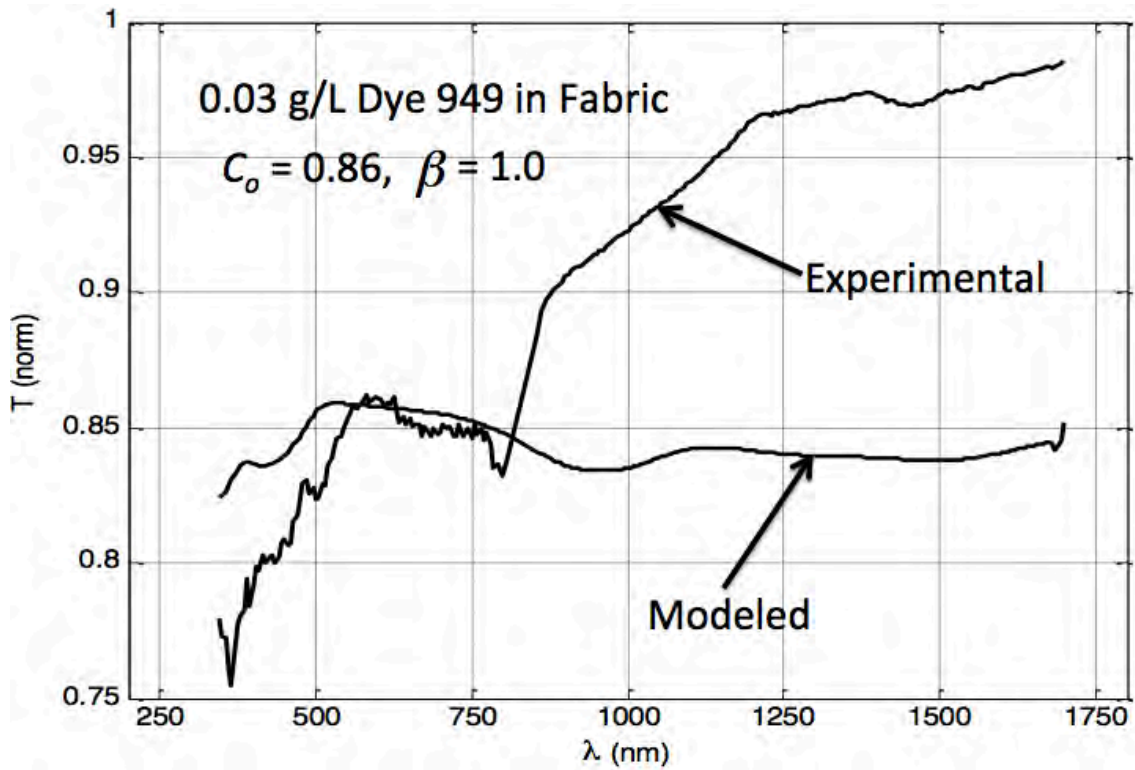


Figure 9a. Comparison of modeled and experimental transmission spectra defined by Eqs. (5) and (6), respectively.

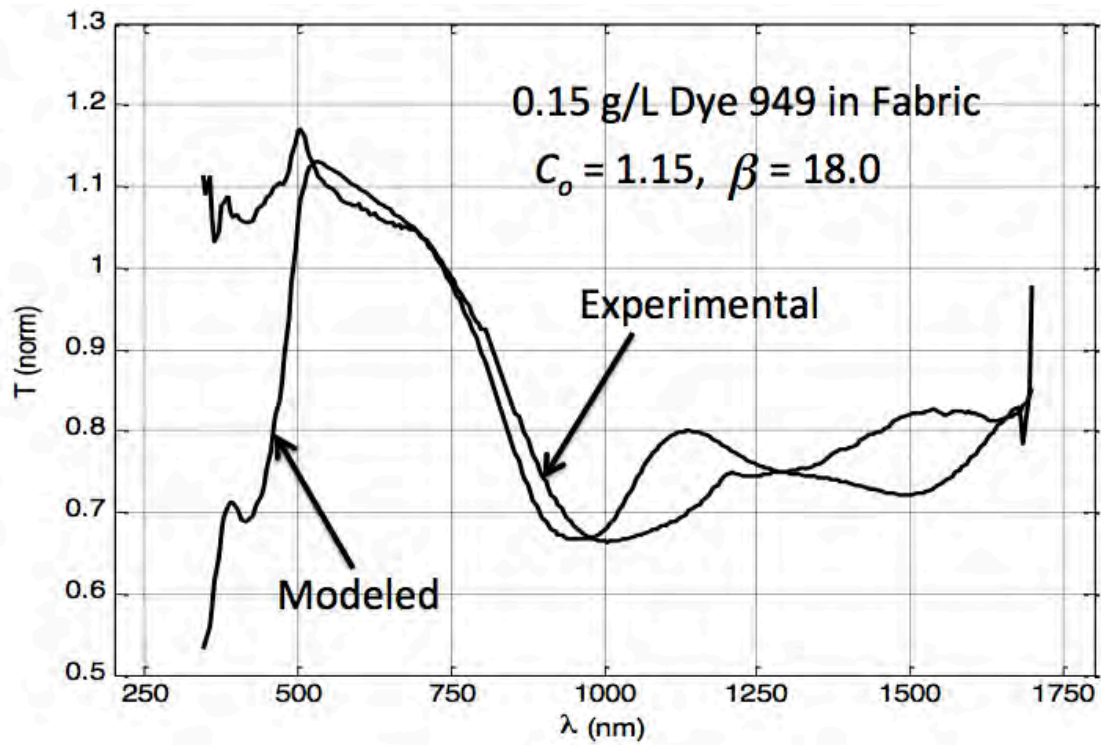


Figure 9b. Comparison of modeled and experimental transmission spectra defined by Eqs. (5) and (6), respectively.

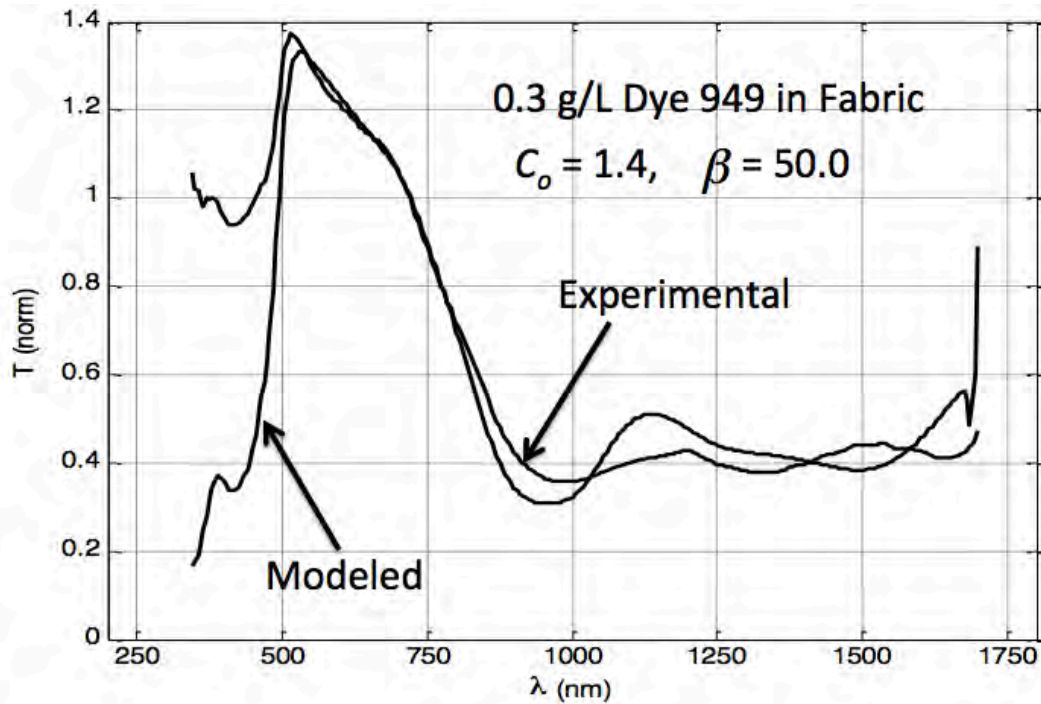


Figure 9c. Comparison of modeled and experimental transmission spectra defined by Eqs. (5) and (6), respectively.

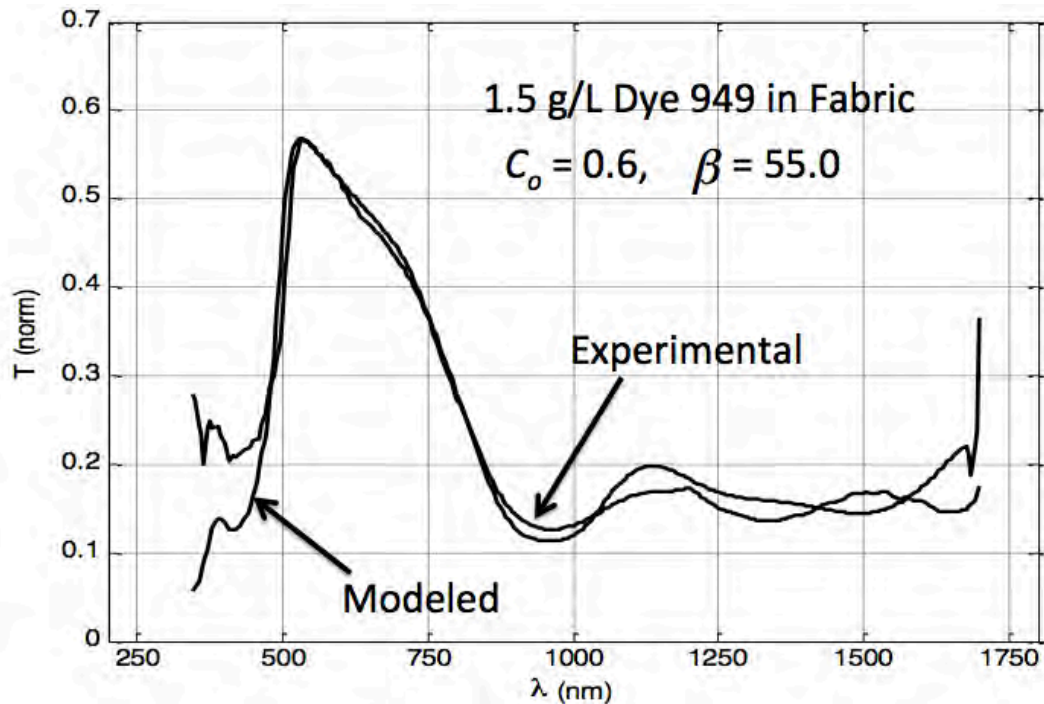


Figure 9d. Comparison of modeled and experimental transmission spectra defined by Eqs. (5) and (6), respectively.

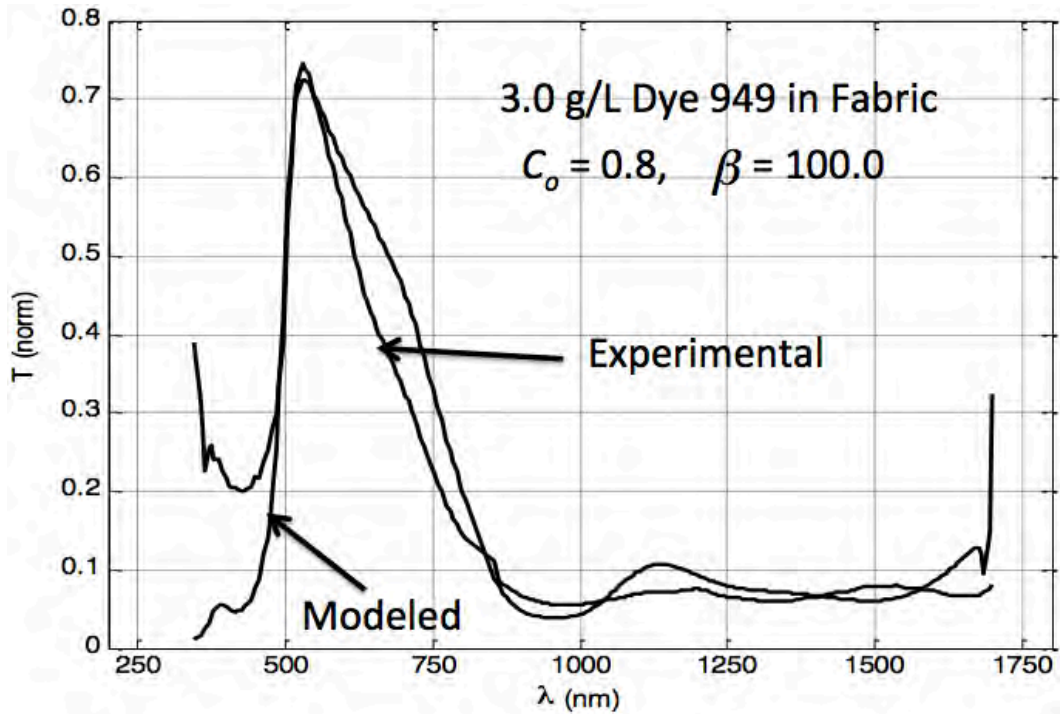


Figure 9e. Comparison of modeled and experimental transmission spectra defined by Eqs. (5) and (6), respectively.

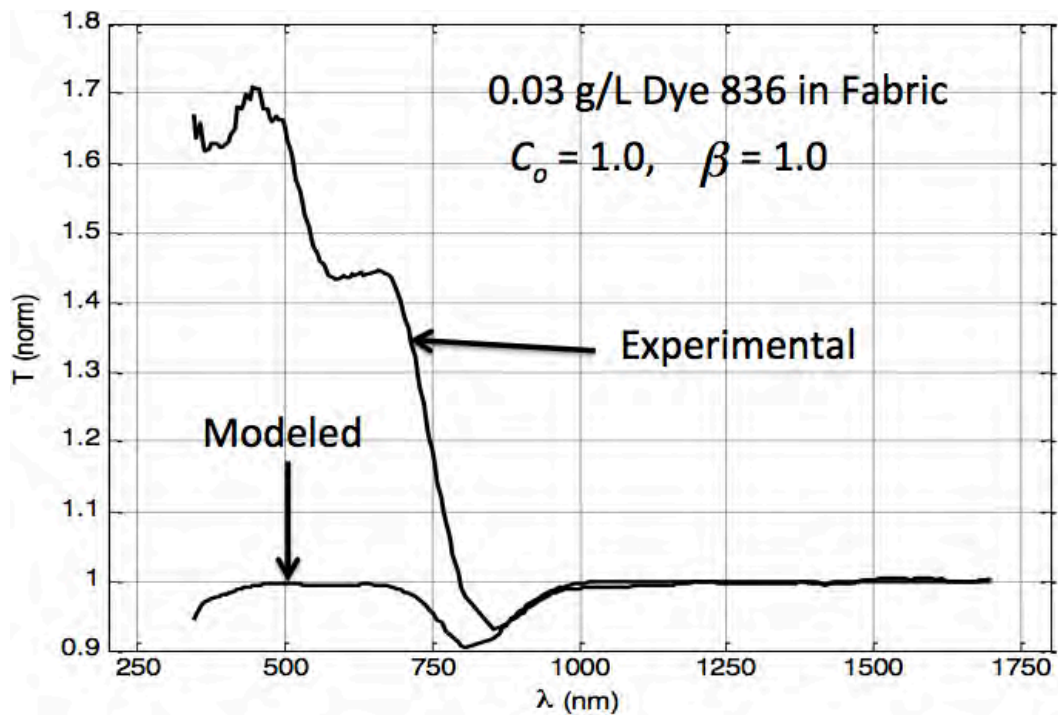


Figure 10a. Comparison of modeled and experimental transmission spectra defined by Eqs. (5) and (6), respectively.

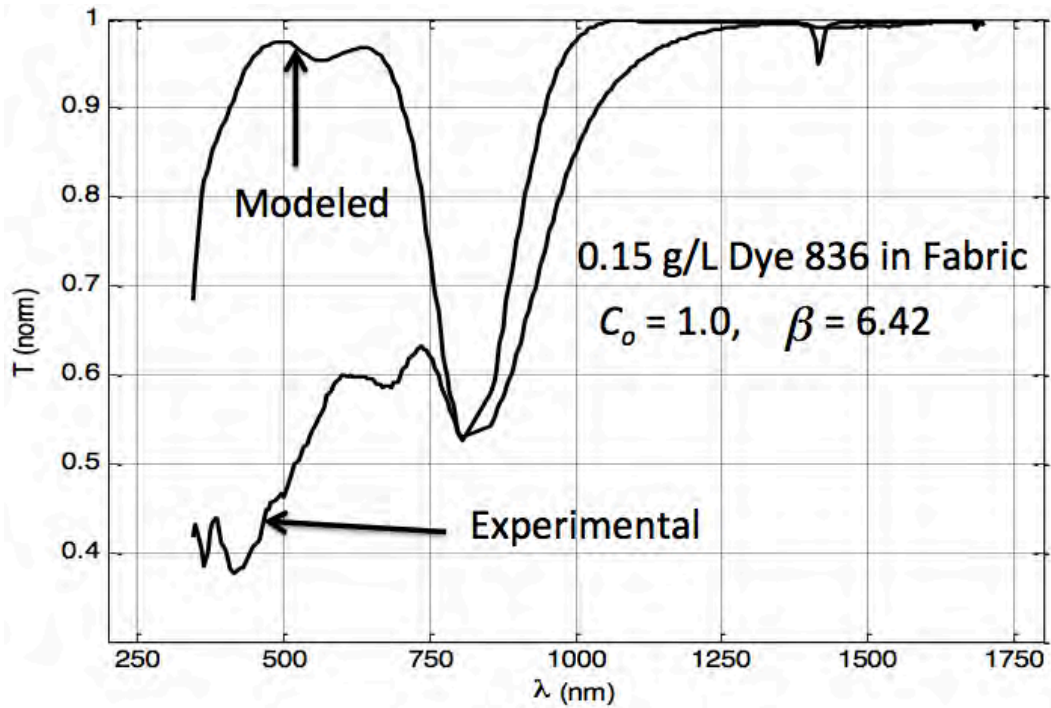


Figure 10b. Comparison of modeled and experimental transmission spectra defined by Eqs. (5) and (6), respectively.

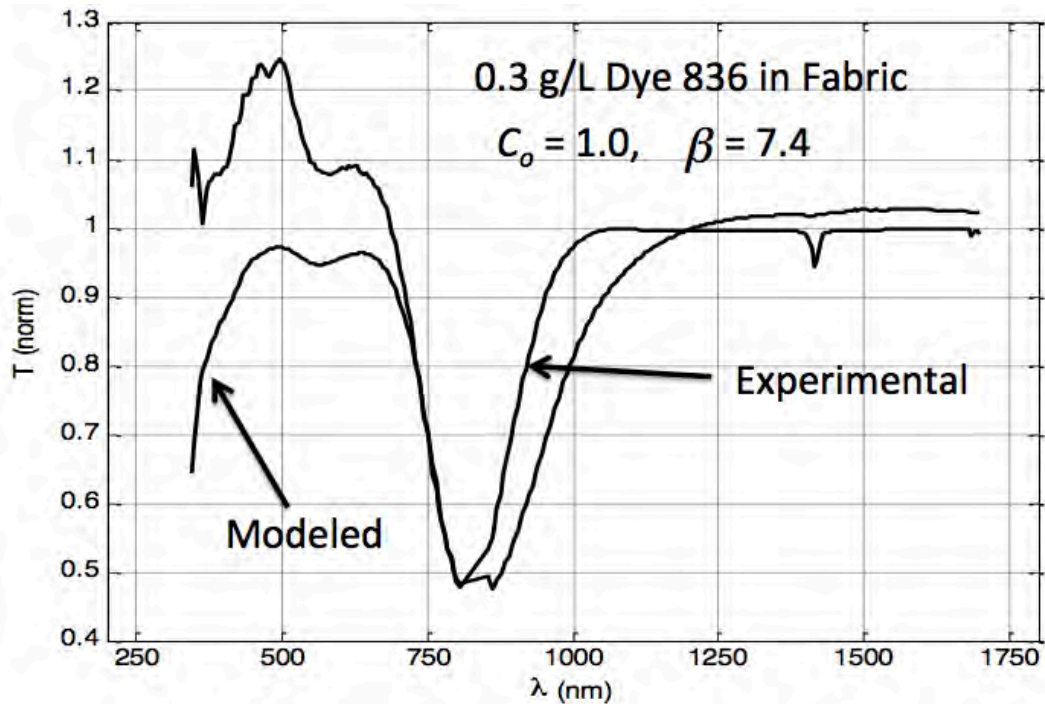


Figure 10c. Comparison of modeled and experimental transmission spectra defined by Eqs. (5) and (6), respectively.

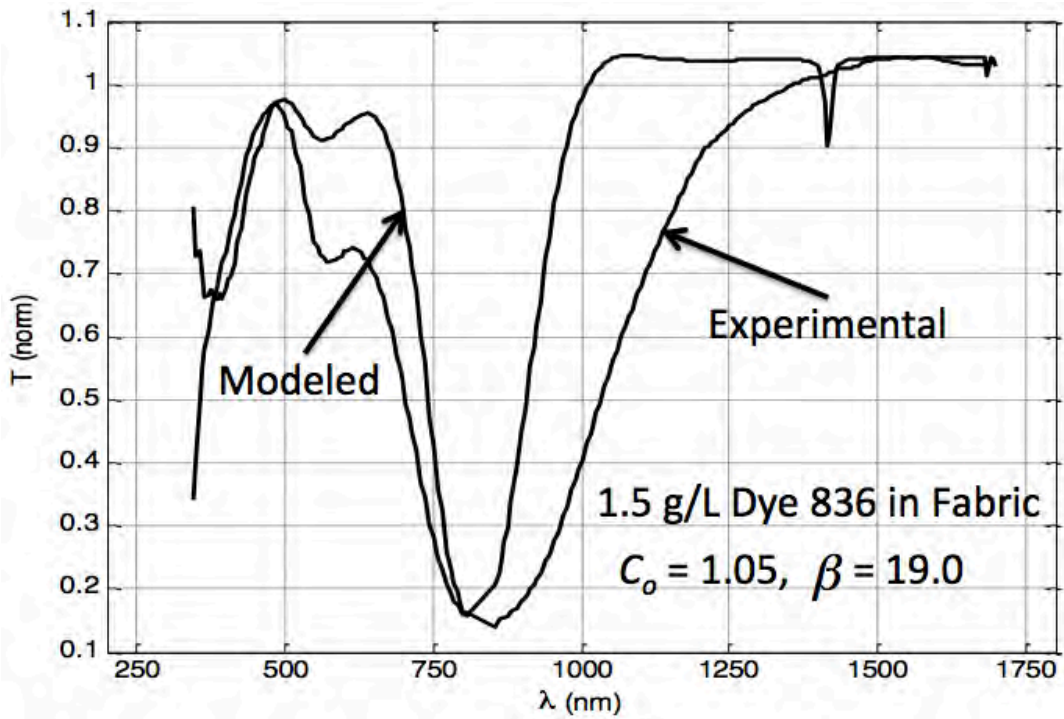


Figure 10d. Comparison of modeled and experimental transmission spectra defined by Eqs. (5) and (6), respectively.

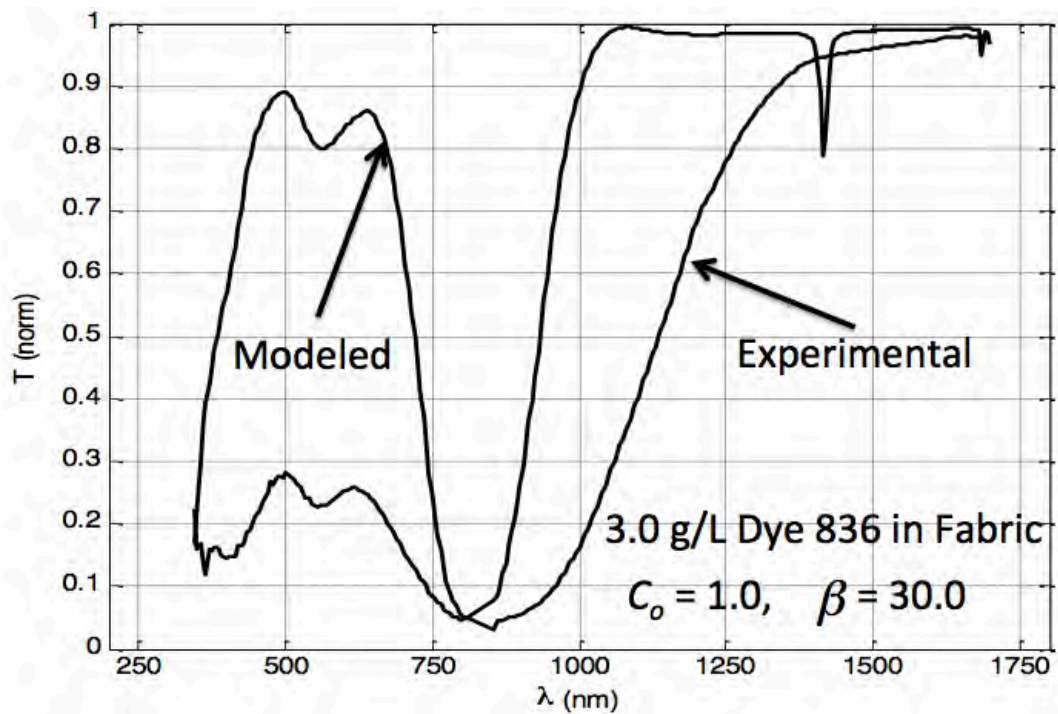


Figure 10e. Comparison of modeled and experimental transmission spectra defined by Eqs. (5) and (6), respectively.

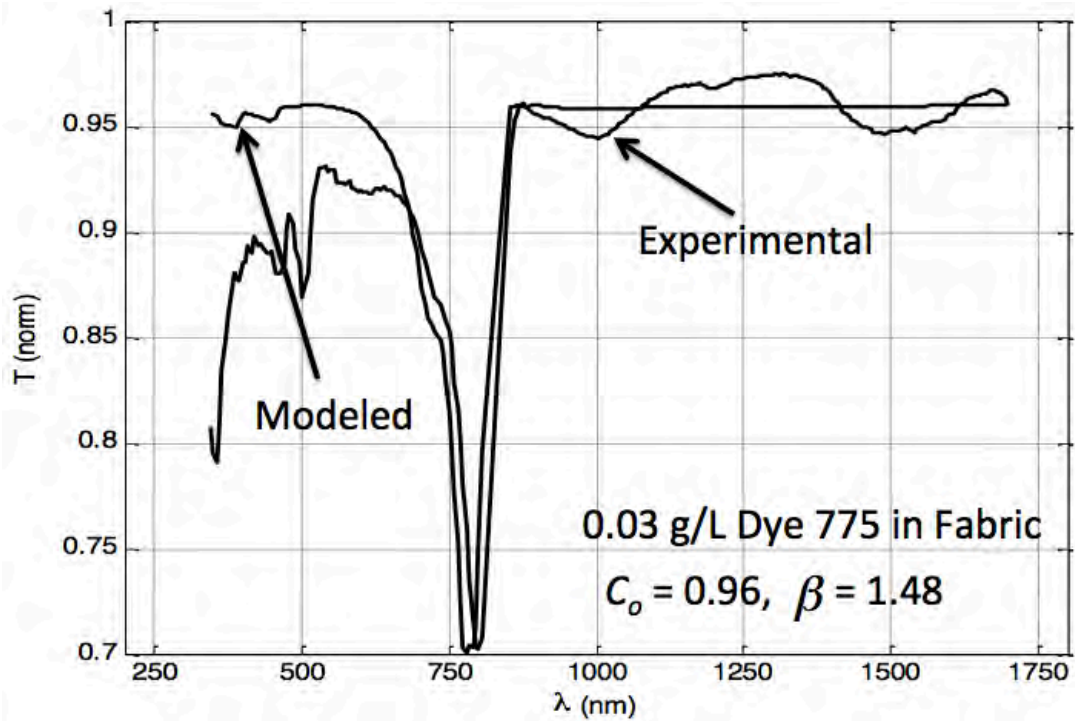


Figure 11a. Comparison of modeled and experimental transmission spectra defined by Eqs. (5) and (6), respectively.

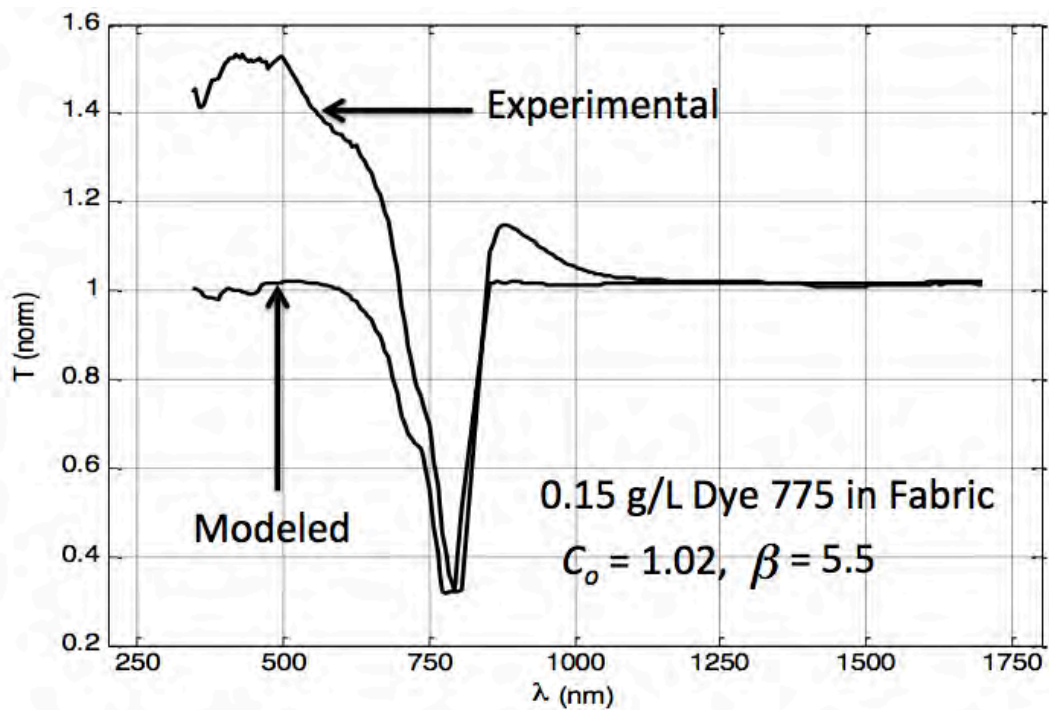


Figure 11b. Comparison of modeled and experimental transmission spectra defined by Eqs. (5) and (6), respectively.

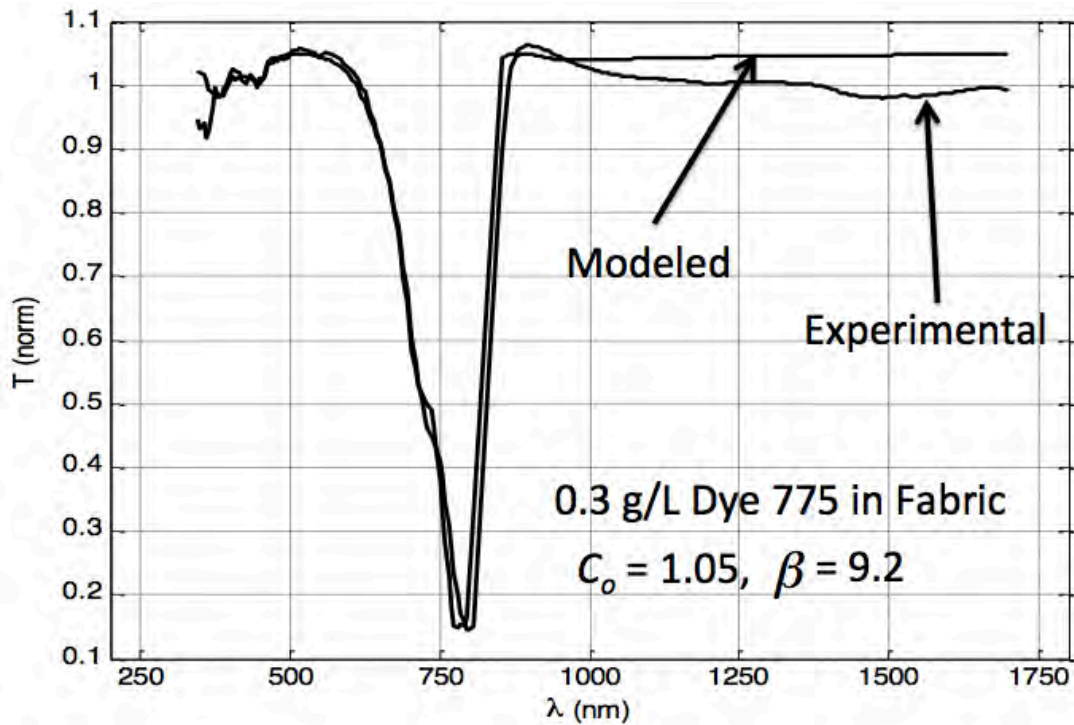


Figure 11c. Comparison of modeled and experimental transmission spectra defined by Eqs. (5) and (6), respectively.

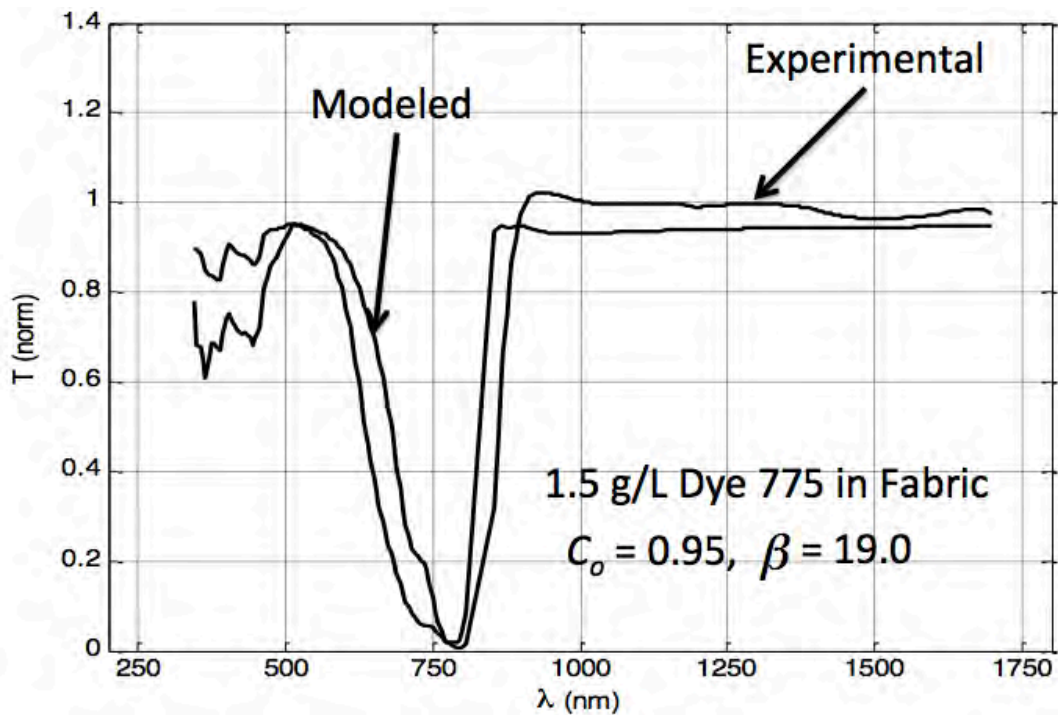


Figure 11d. Comparison of modeled and experimental transmission spectra defined by Eqs. (5) and (6), respectively.

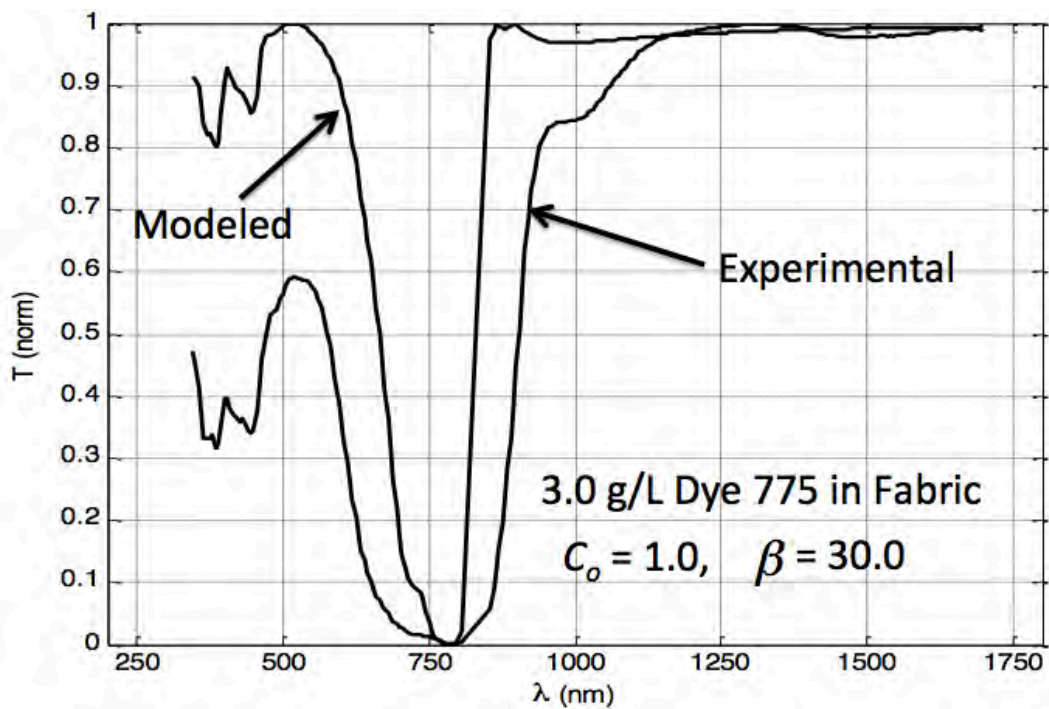


Figure 11e. Comparison of modeled and experimental transmission spectra defined by Eqs. (5) and (6), respectively.

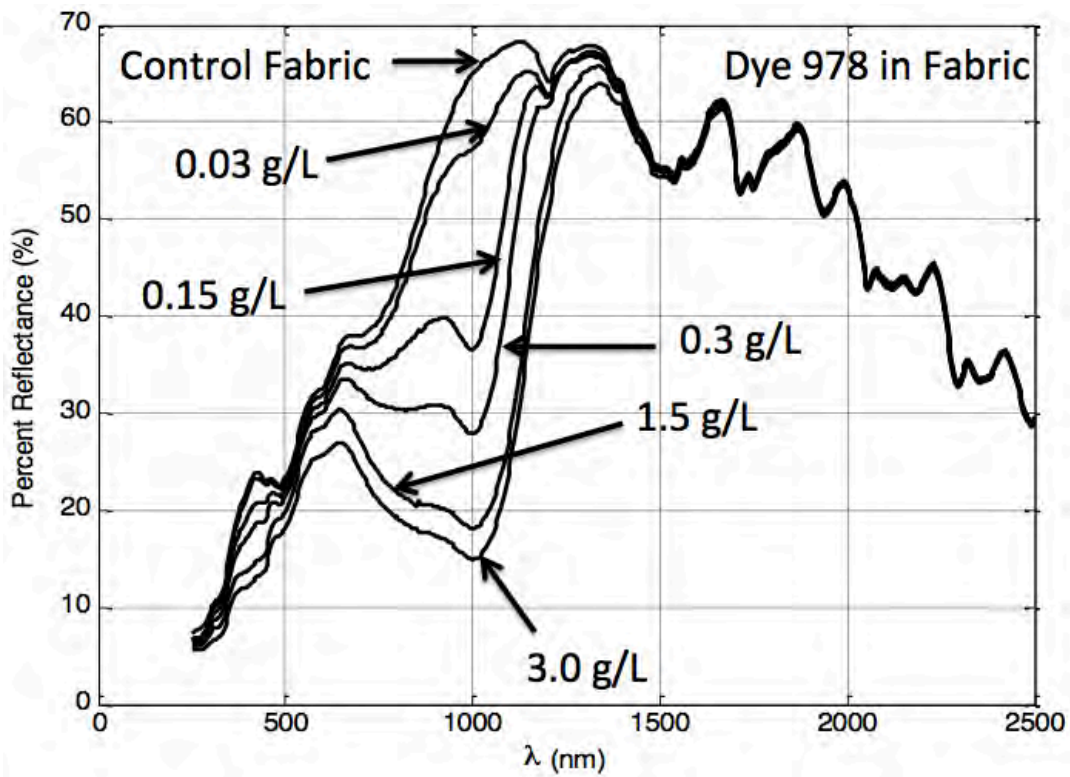


Figure 12. Experimentally measured reflectance spectra for fabric with and without Triarylamine dye embedded as a function of dye concentration.

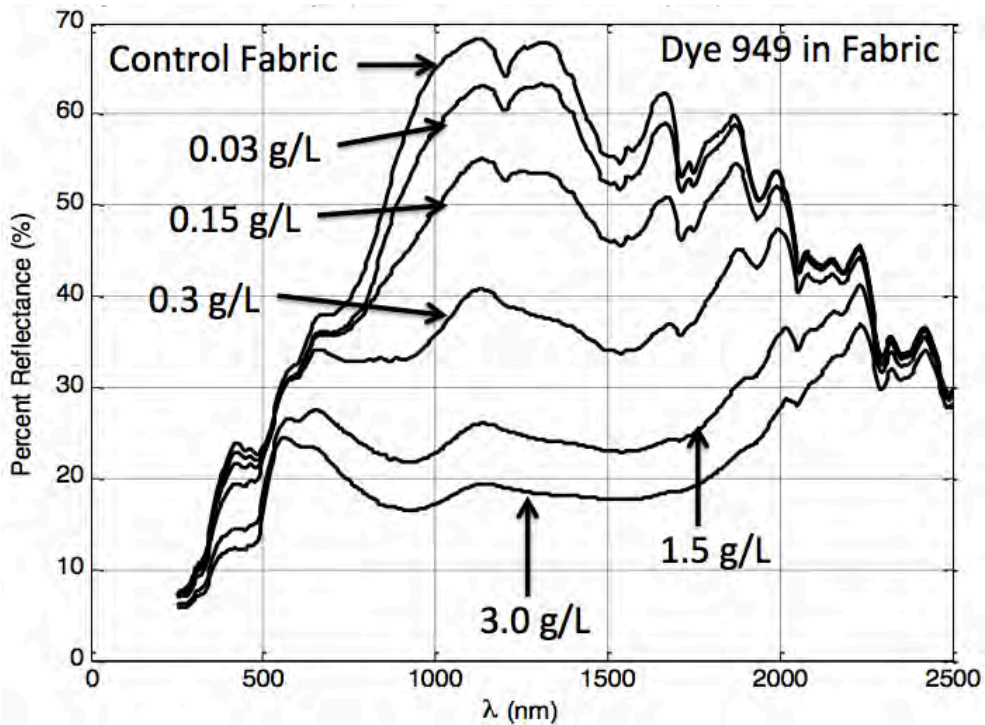


Figure 13. Experimentally measured reflectance spectra for fabric with and without Tetraaryldiamine dye embedded as a function of dye concentration.

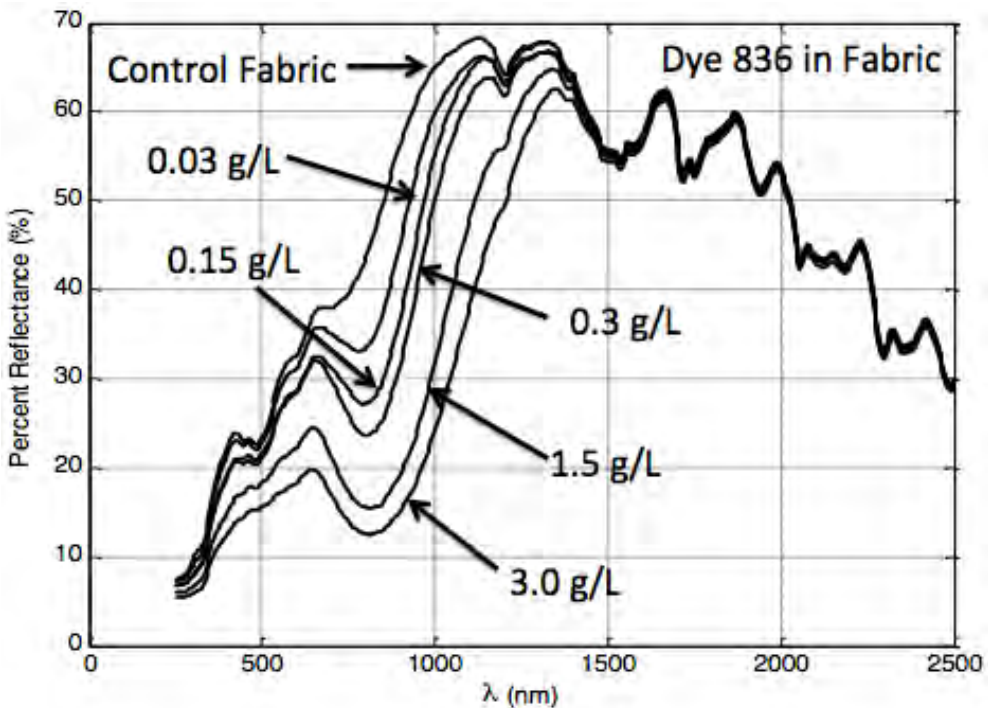


Figure 14. Experimentally measured reflectance spectra for fabric with and without Transition Metal Dithiolene dye embedded as a function of dye concentration.

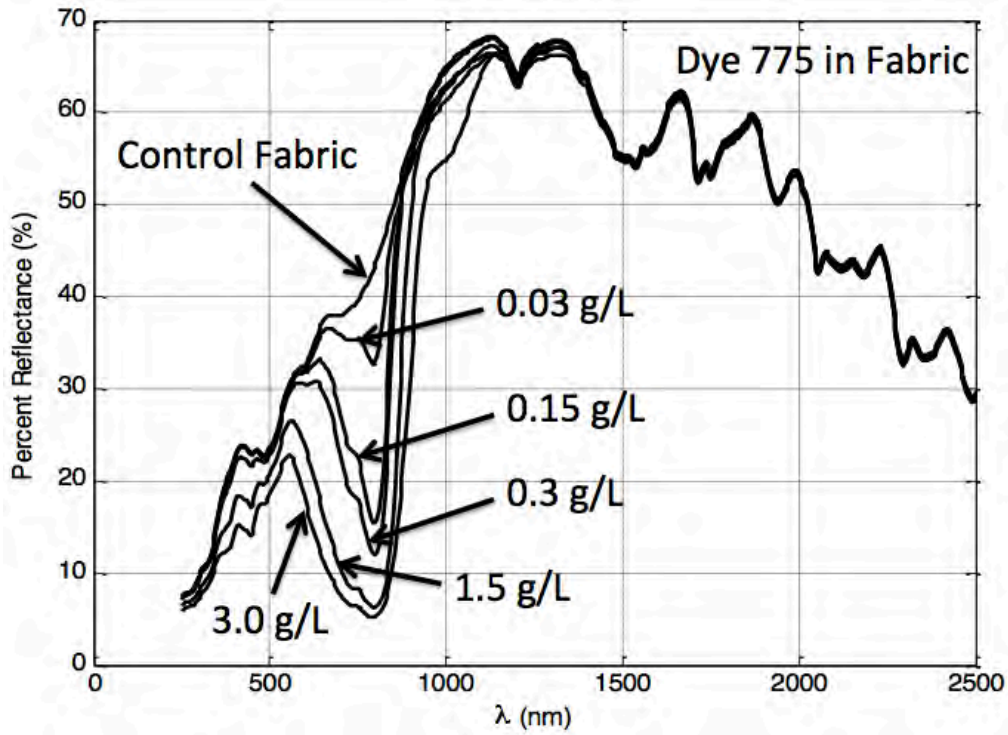


Figure 15. Experimentally measured reflectance spectra for fabric with and without Indolium Iodide dye embedded as a function of dye concentration.

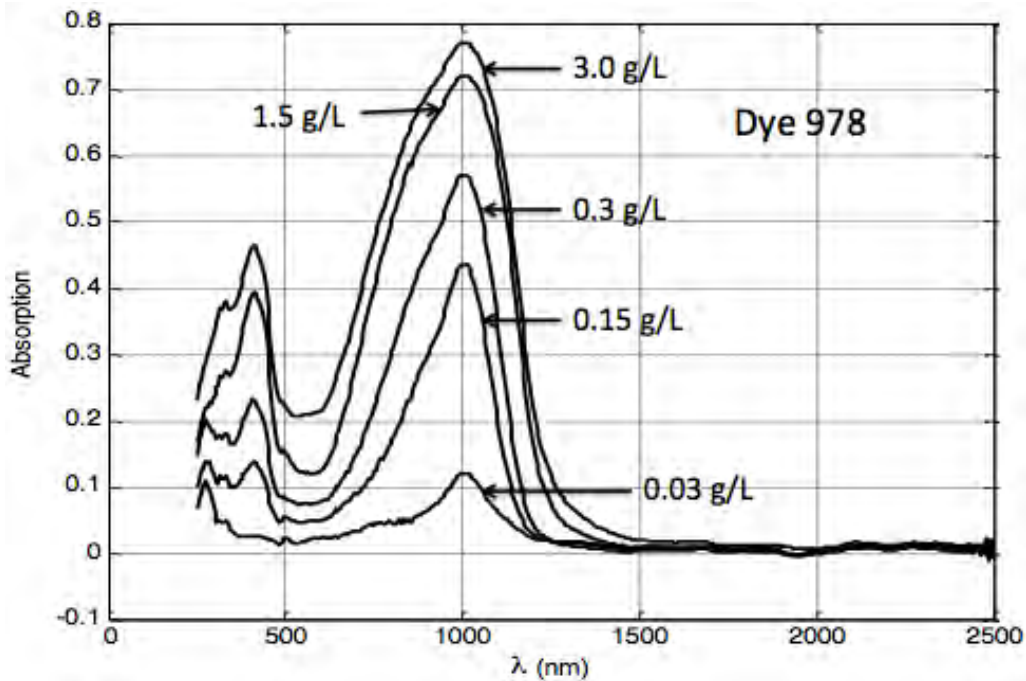


Figure 16. Scaled absorption coefficient defined by Eq. (7) as a function of Triarylamine dye concentration.

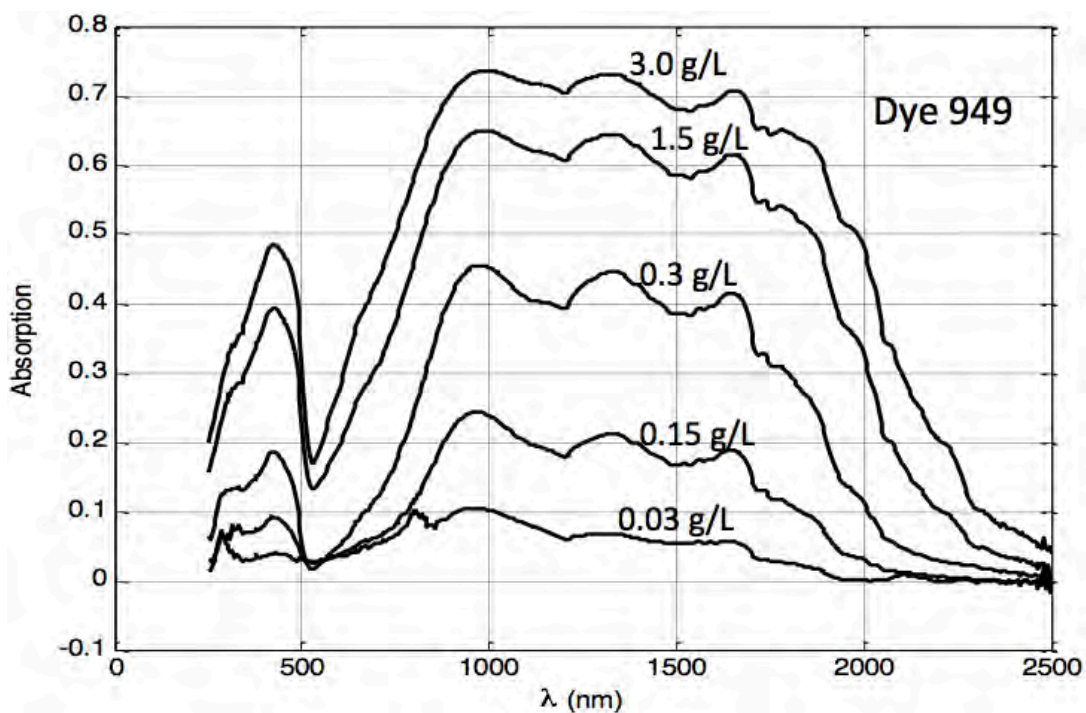


Figure 17. Scaled absorption coefficient defined by Eq. (7) as a function of Tetraaryldiamine dye concentration.

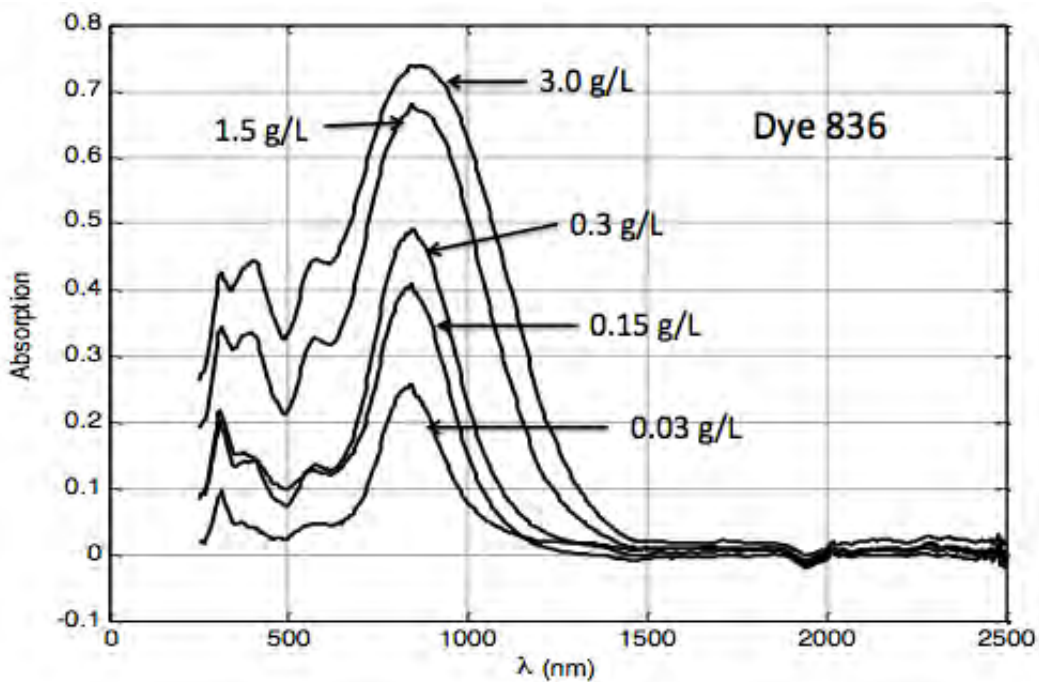


Figure 18. Scaled absorption coefficient defined by Eq. (7) as a function of Transition Metal Dithiolene dye concentration.

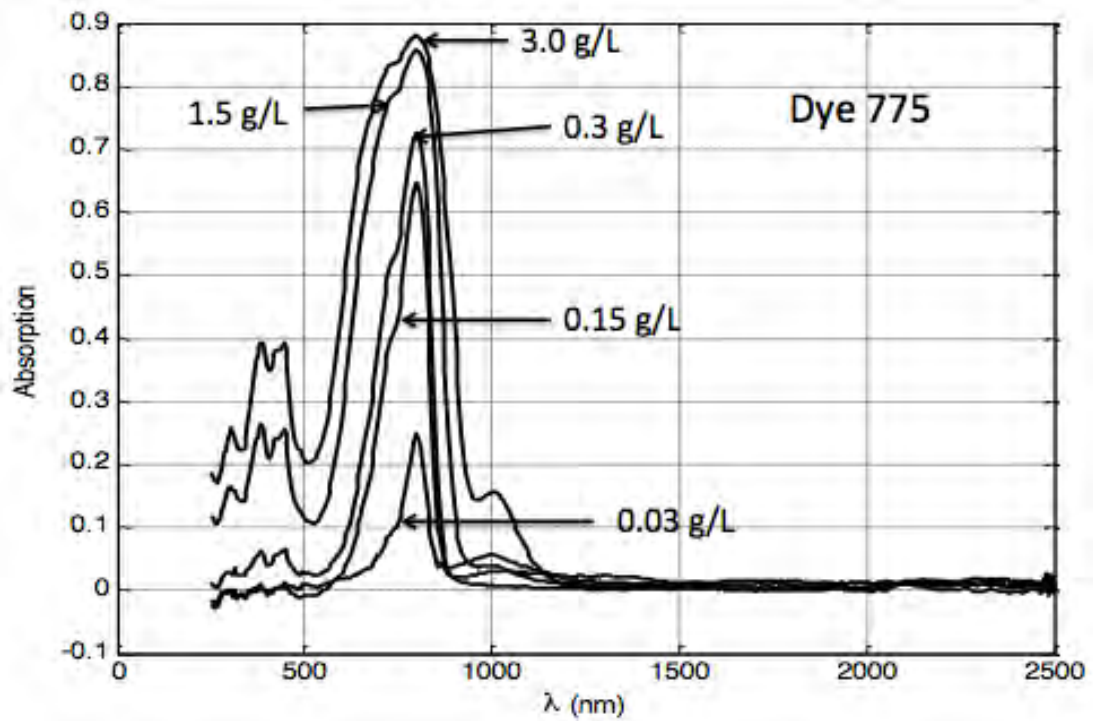


Figure 19. Scaled absorption coefficient defined by Eq. (7) as a function of Indolium Iodide dye concentration.

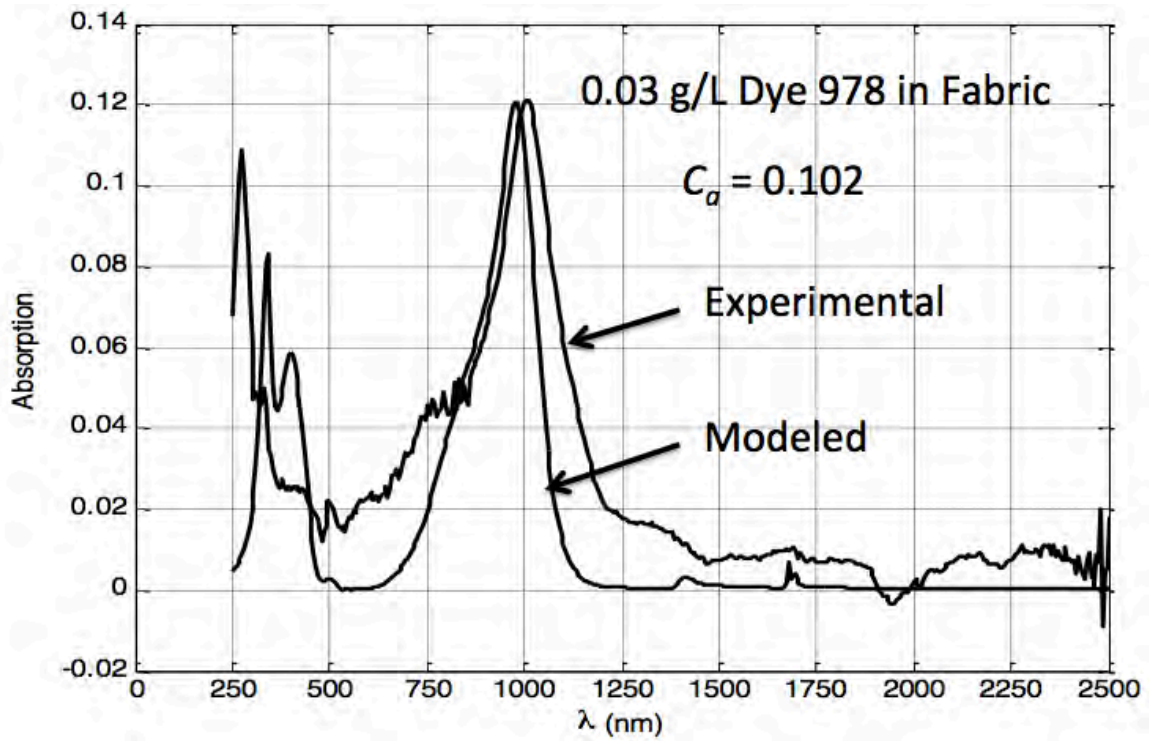


Figure 20a. Comparison of measured and modeled absorption spectra.

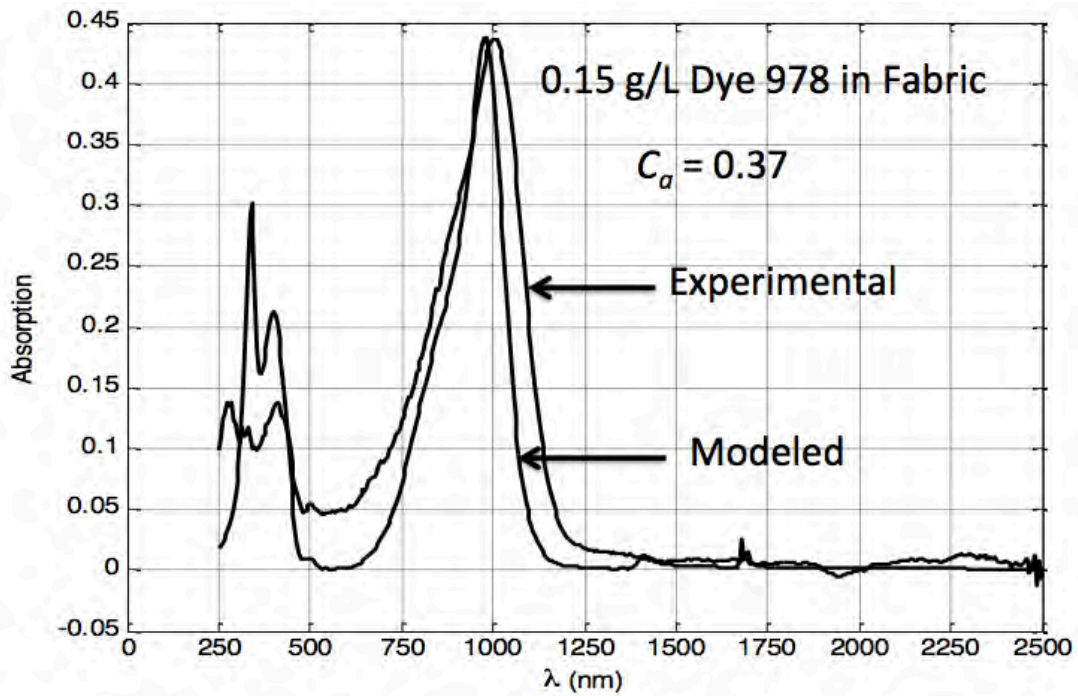


Figure 20b. Comparison of measured and modeled absorption spectra.

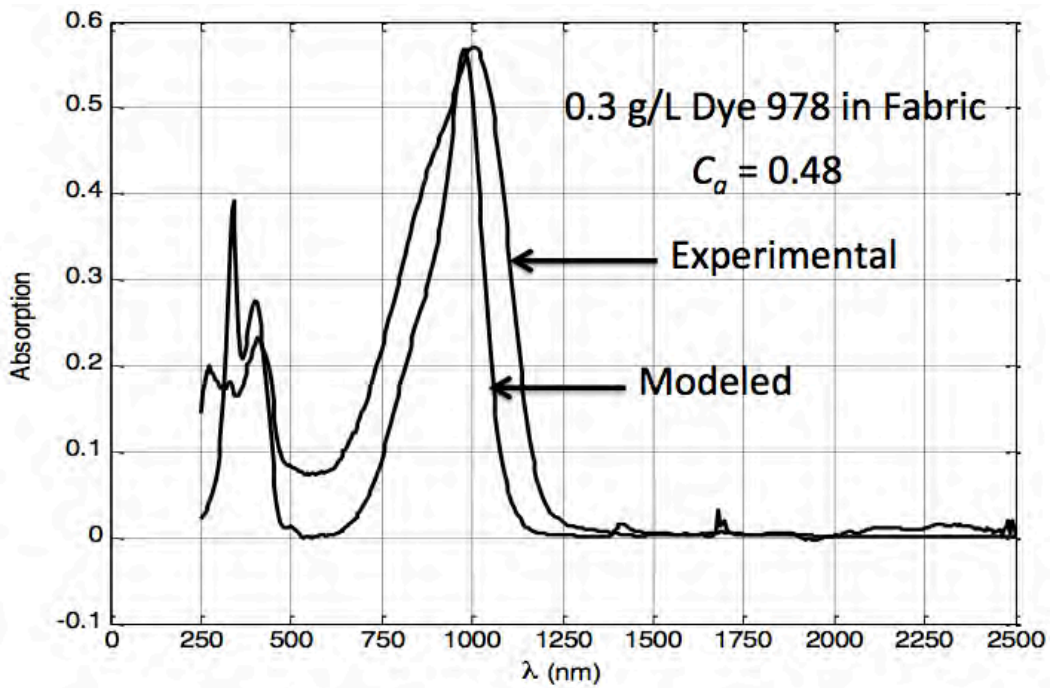


Figure 20c. Comparison of measured and modeled absorption spectra.

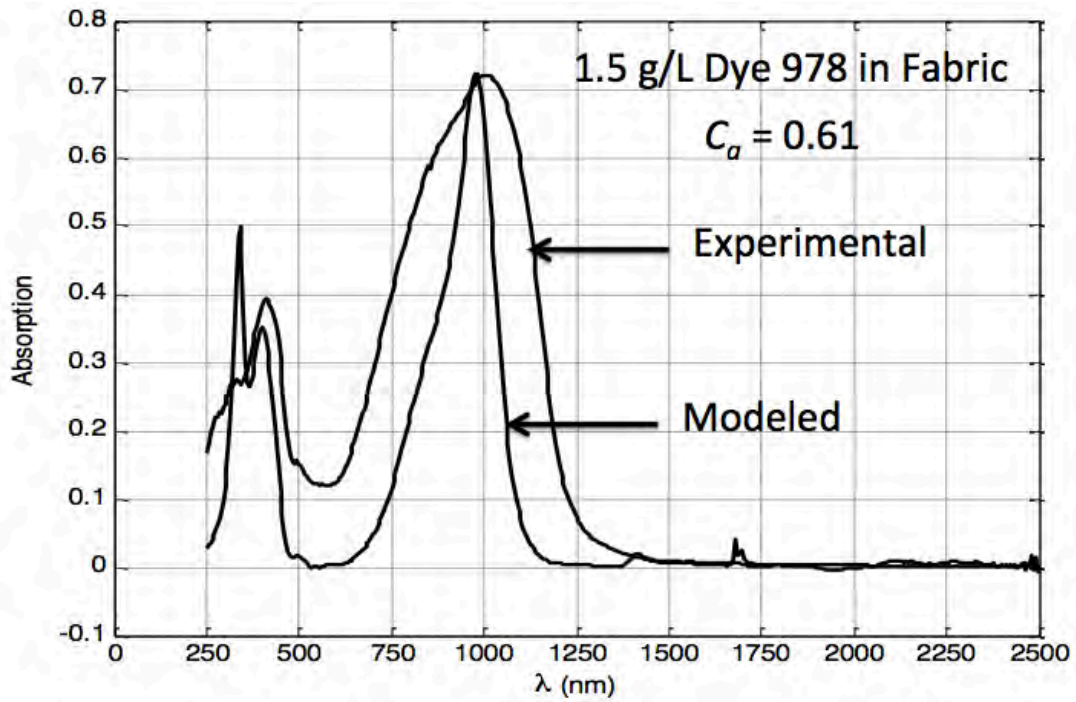


Figure 20d. Comparison of measured and modeled absorption spectra.

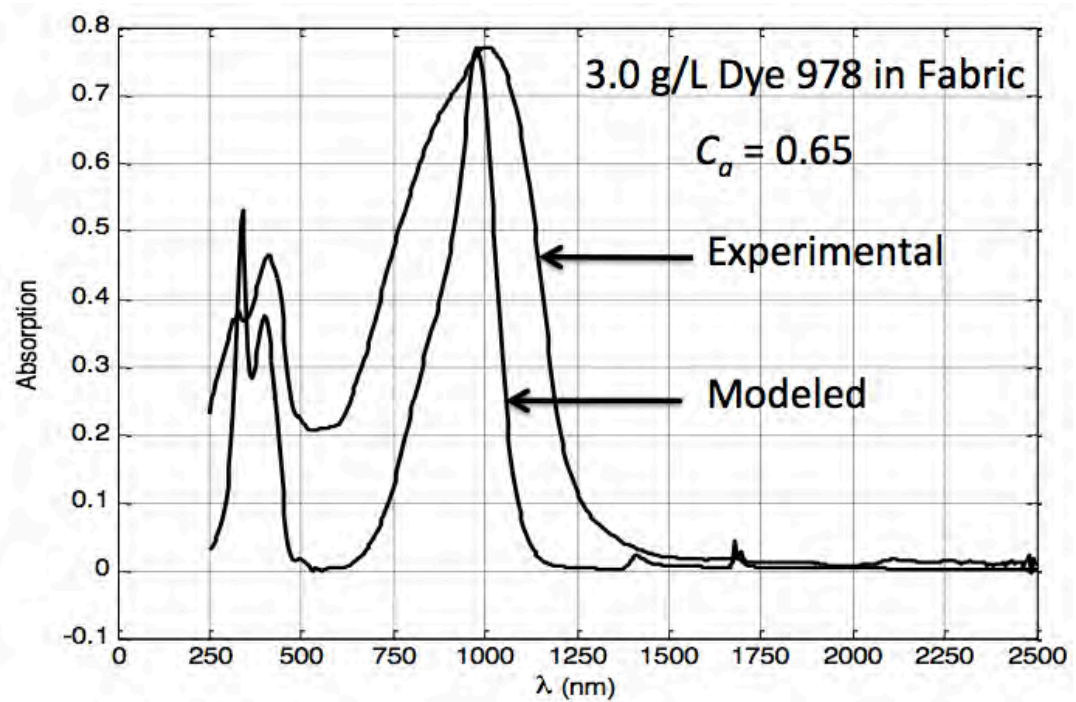


Figure 20e. Comparison of measured and modeled absorption spectra.

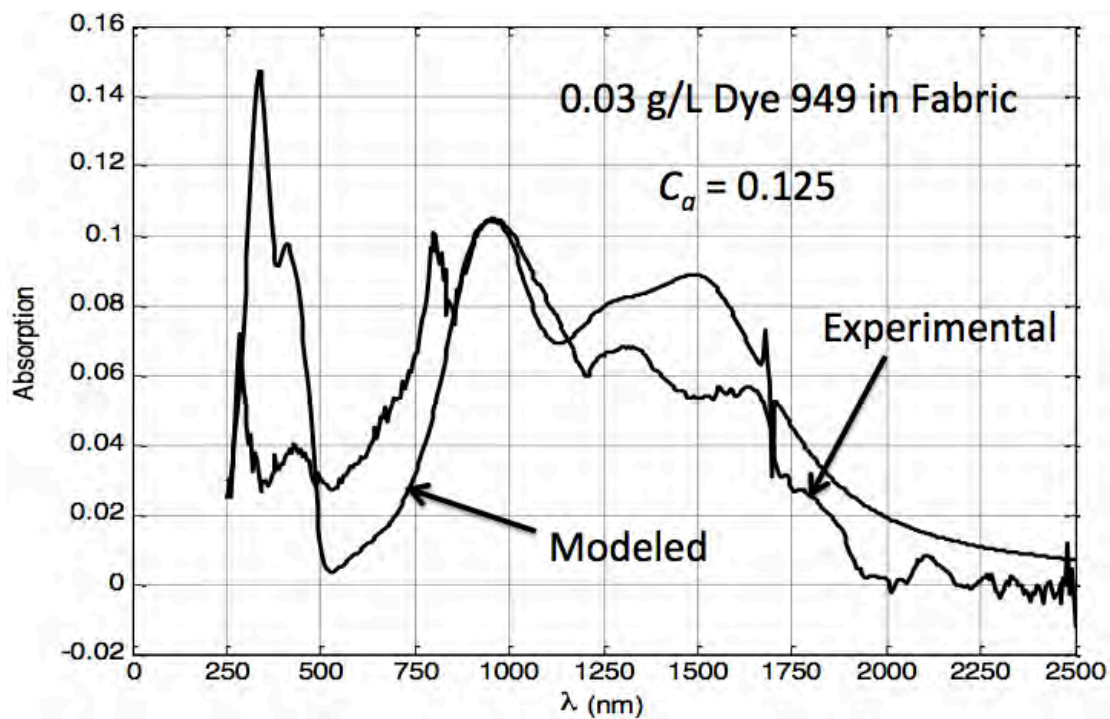


Figure 21a. Comparison of measured and modeled absorption spectra.

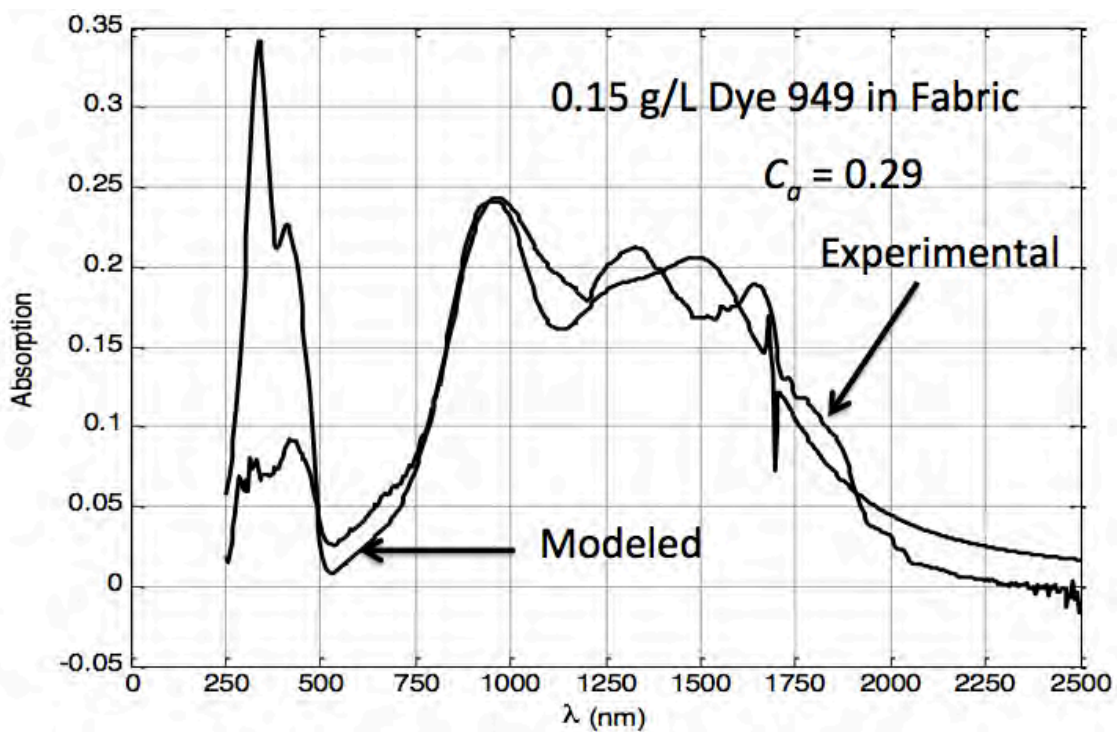


Figure 21b. Comparison of measured and modeled absorption spectra.

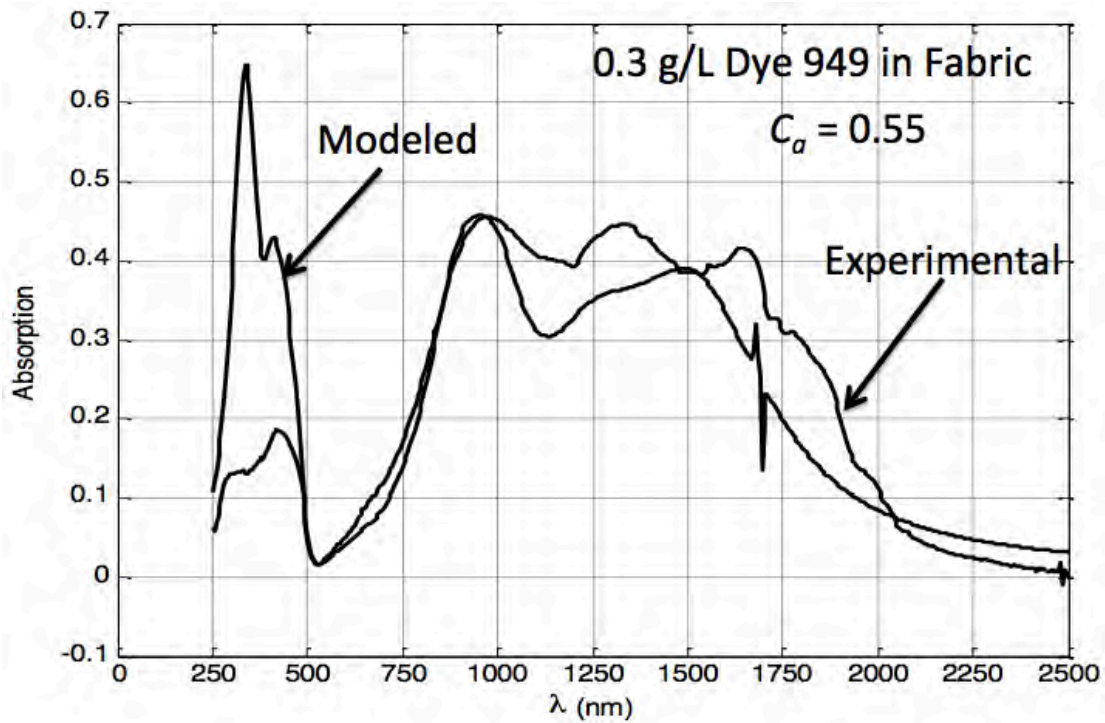


Figure 21c. Comparison of measured and modeled absorption spectra.

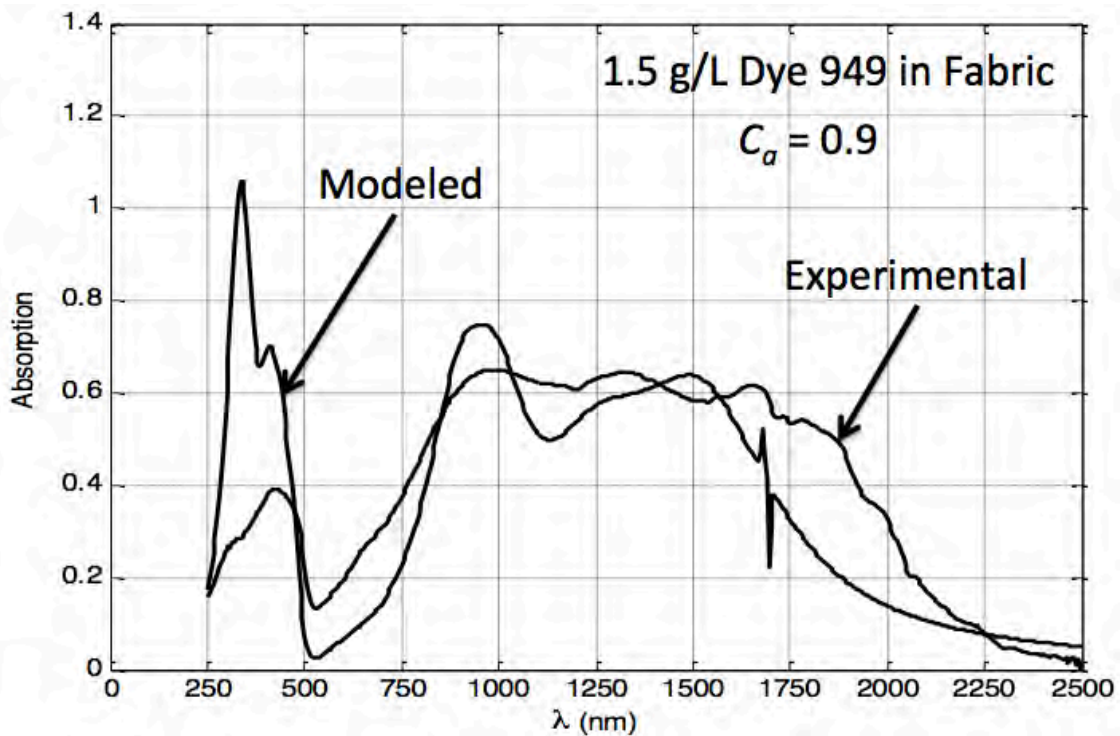


Figure 21d. Comparison of measured and modeled absorption spectra.

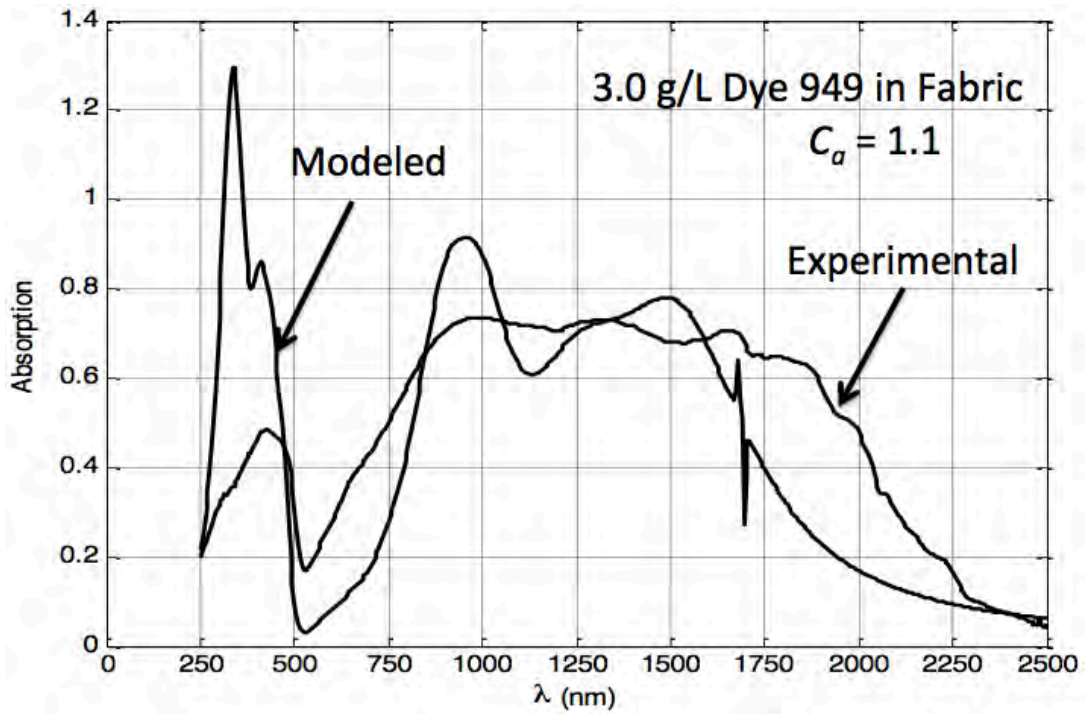


Figure 21e. Comparison of measured and modeled absorption spectra.

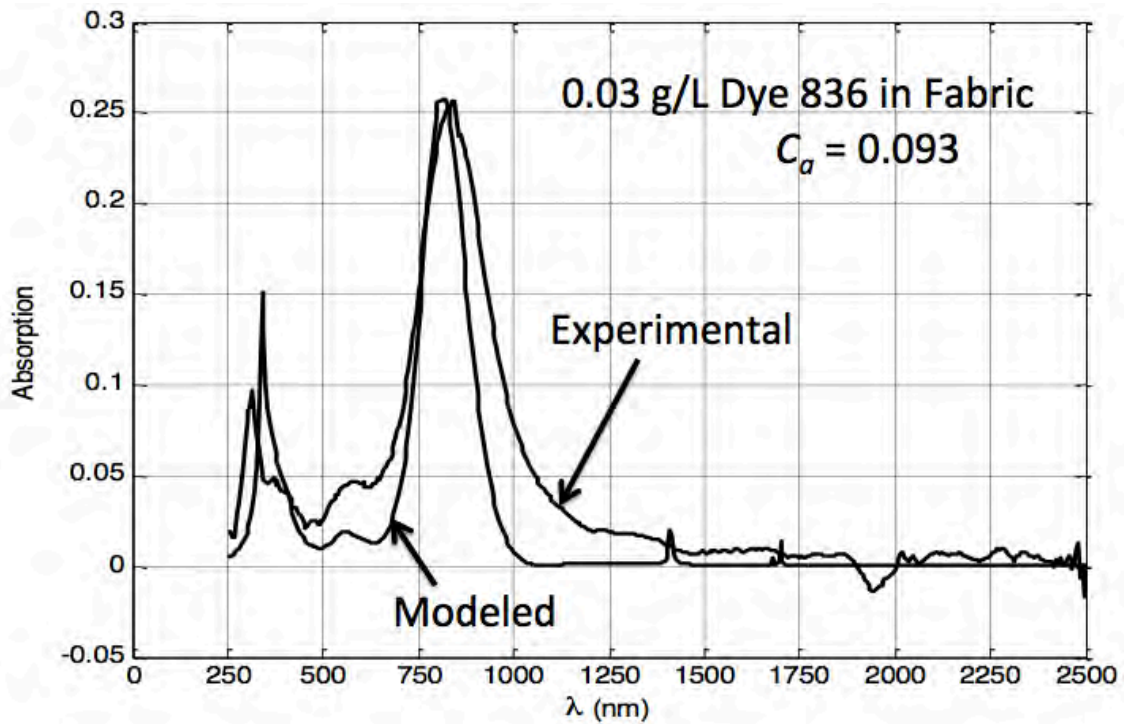


Figure 22a. Comparison of measured and modeled absorption spectra.

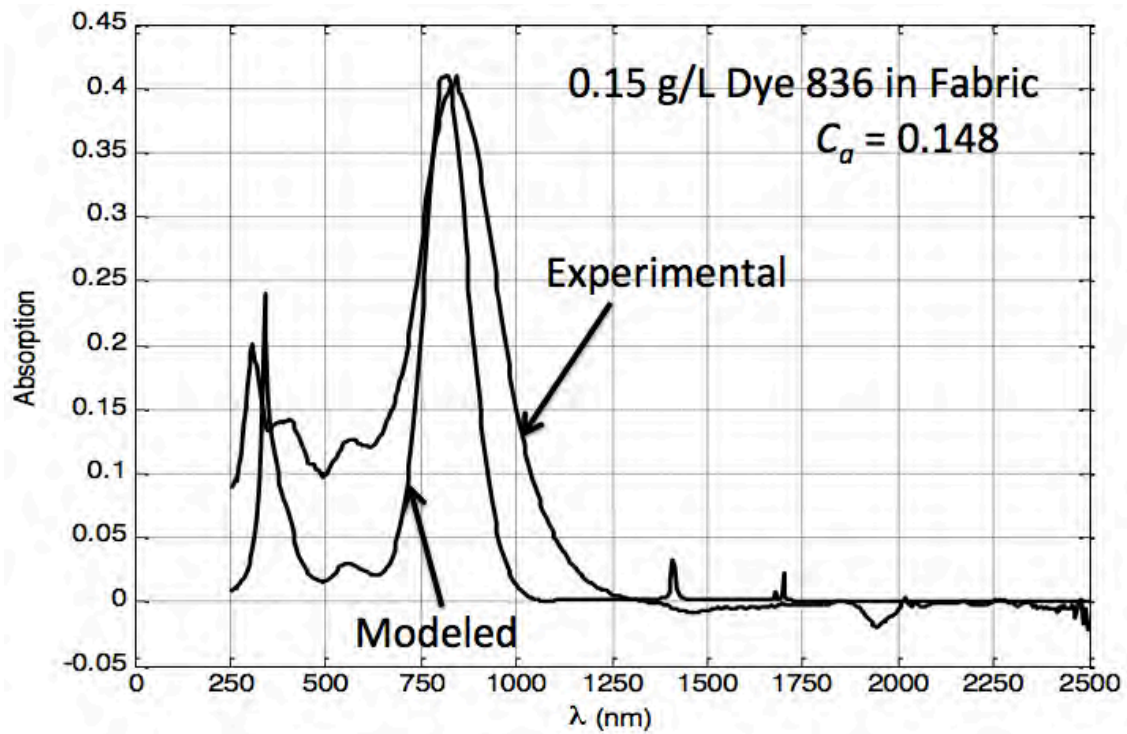


Figure 22b. Comparison of measured and modeled absorption spectra.

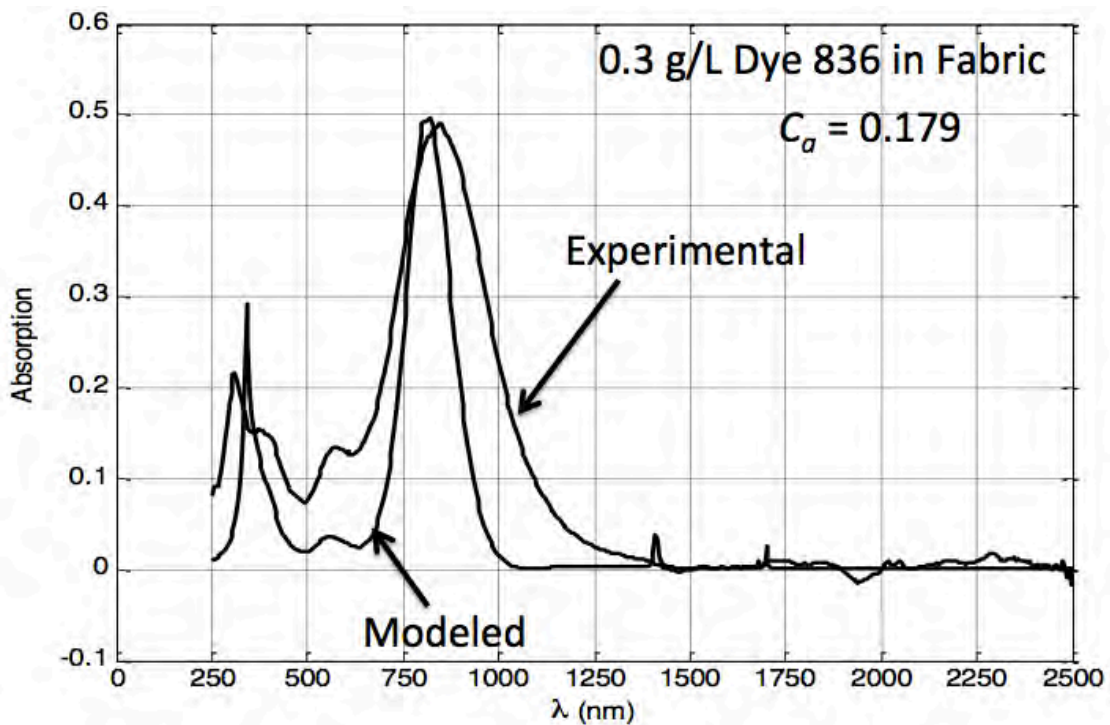


Figure 22c. Comparison of measured and modeled absorption spectra.

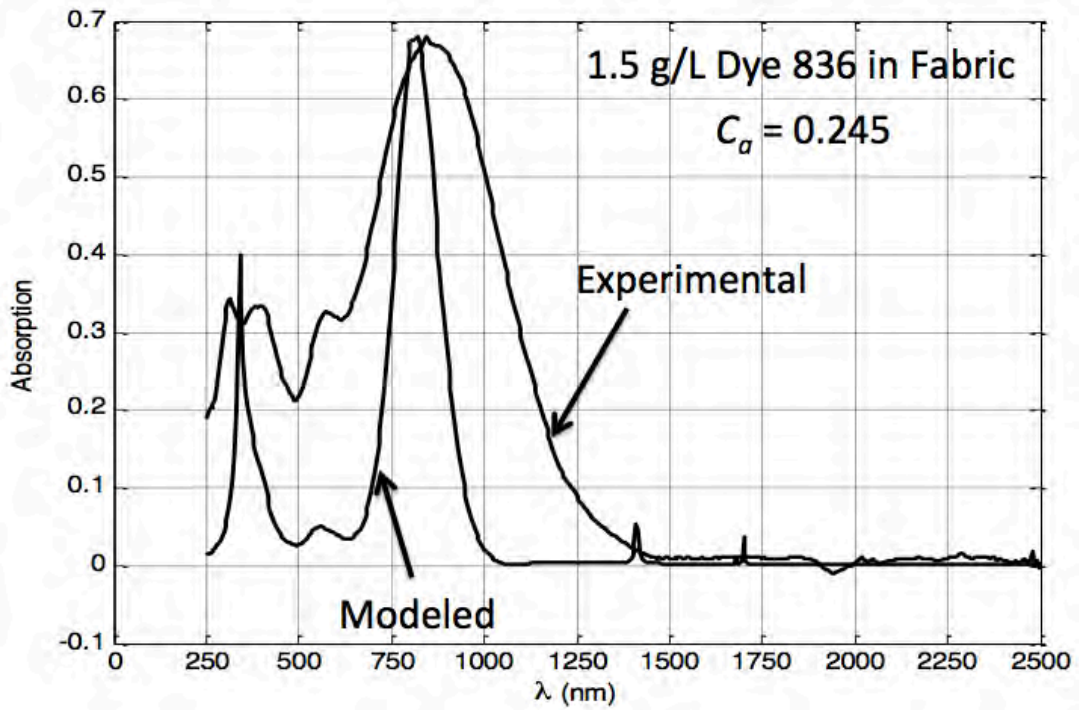


Figure 22d. Comparison of measured and modeled absorption spectra.

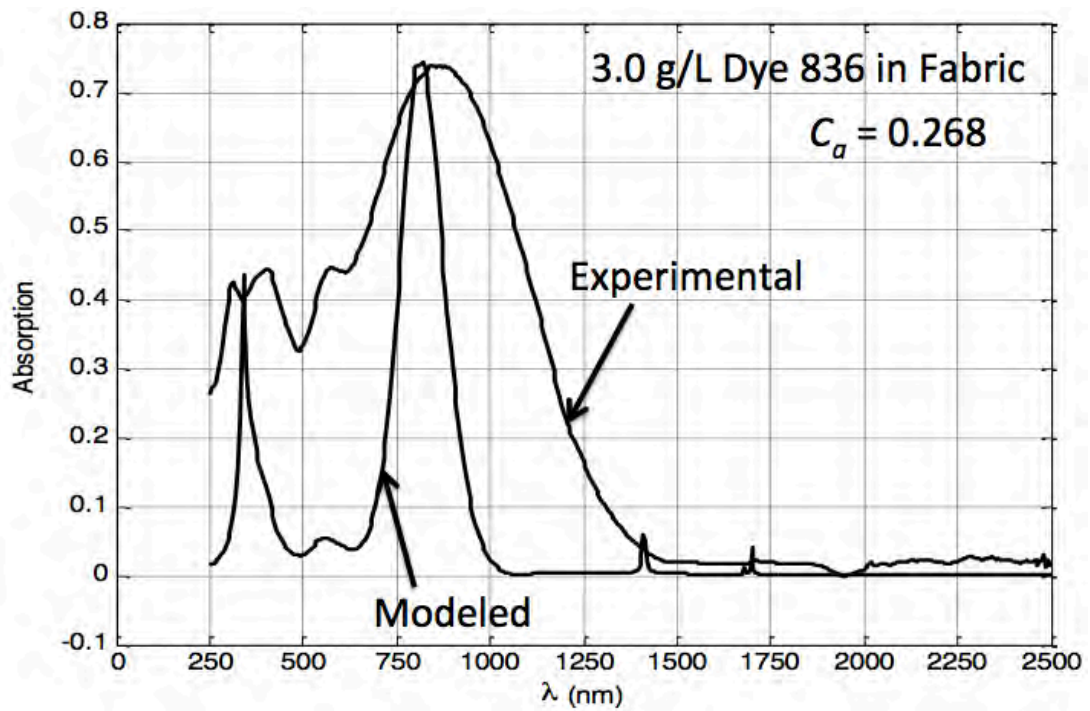


Figure 22e. Comparison of measured and modeled absorption spectra.

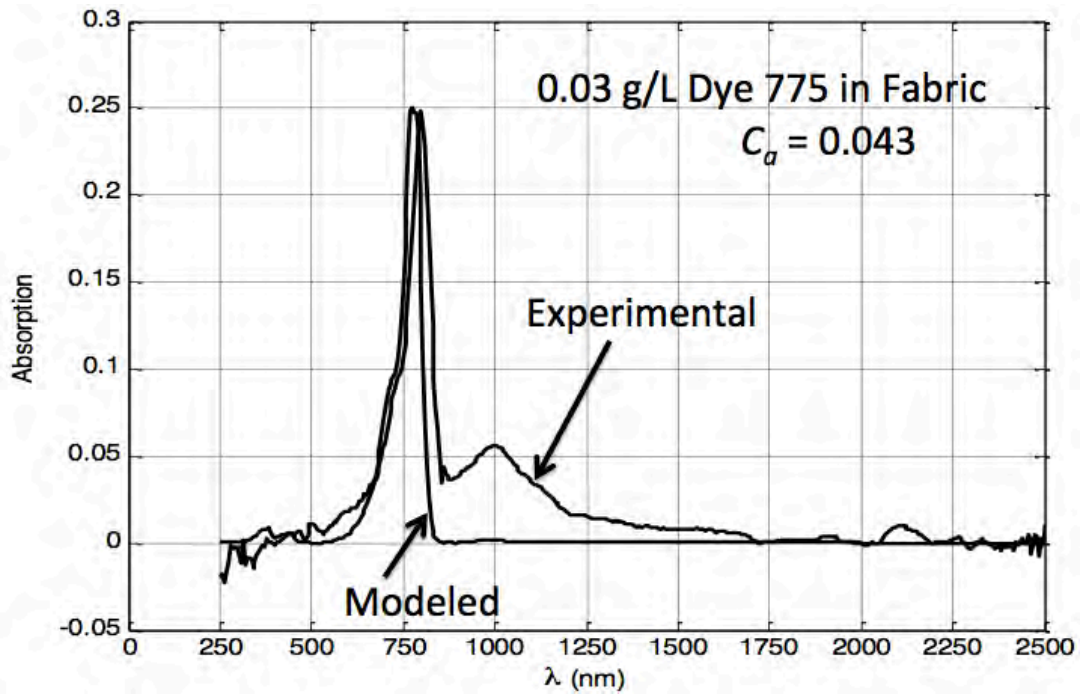


Figure 23a. Comparison of measured and modeled absorption spectra.

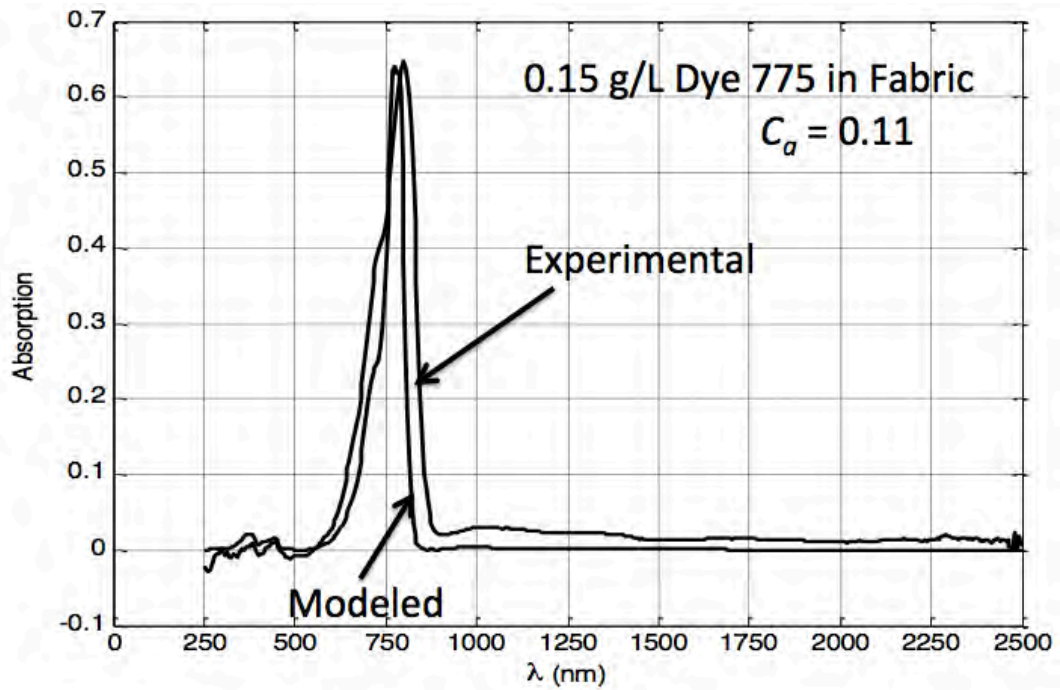


Figure 23b. Comparison of measured and modeled absorption spectra.

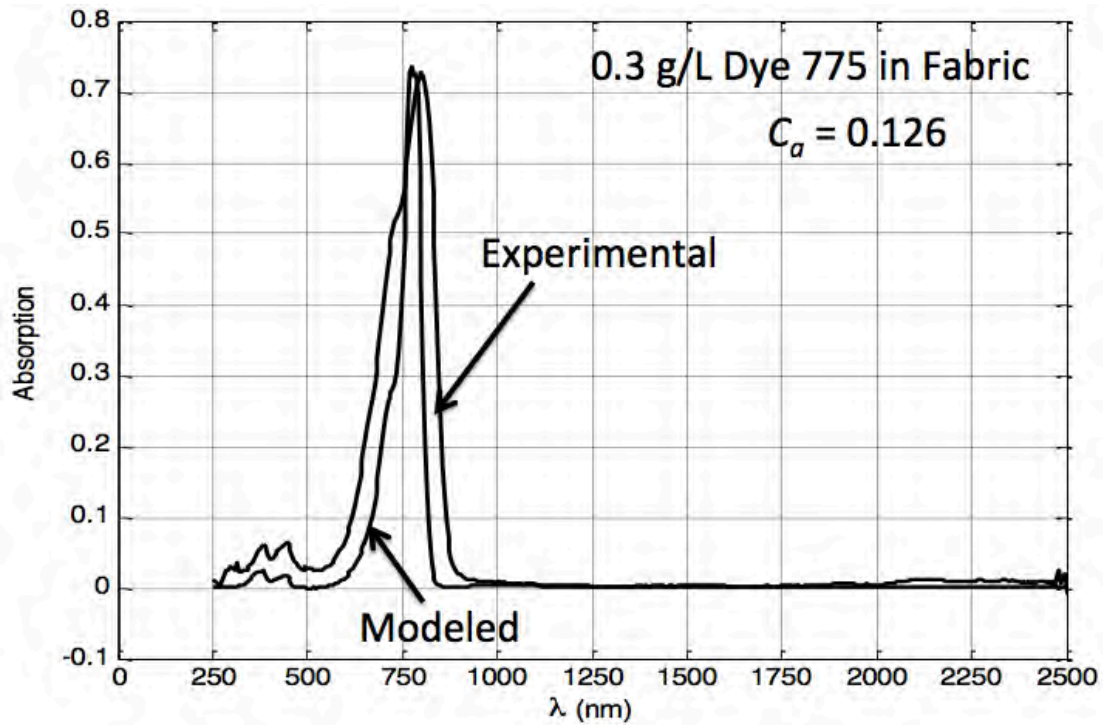


Figure 23c. Comparison of measured and modeled absorption spectra.

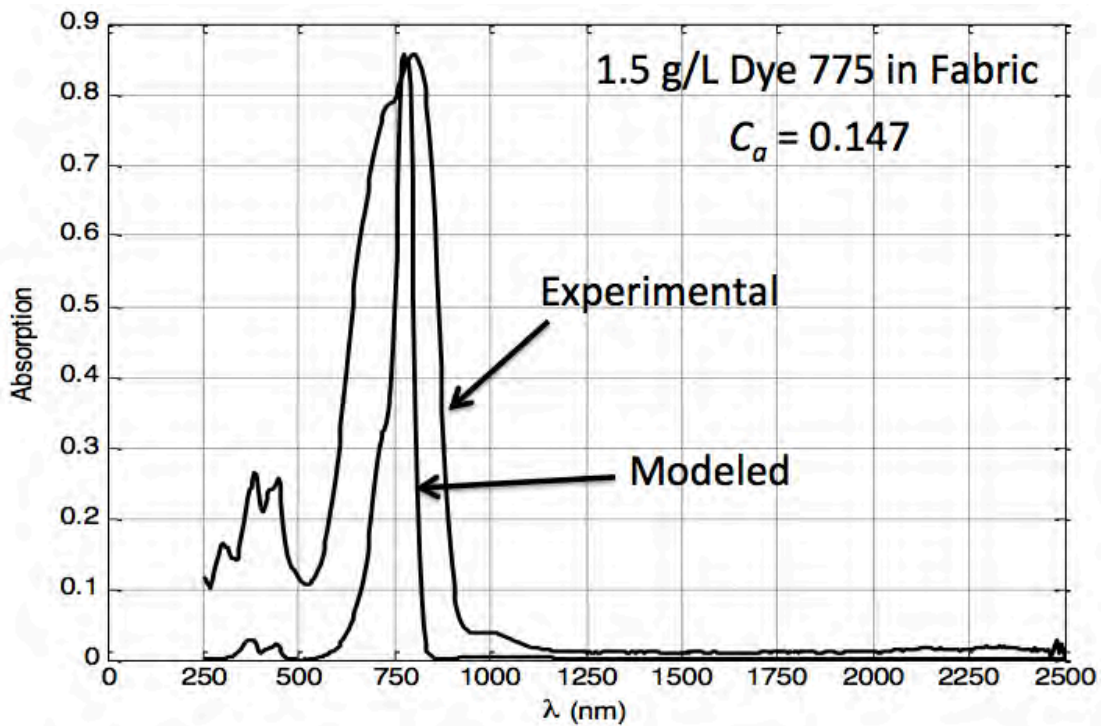


Figure 23d. Comparison of measured and modeled absorption spectra.

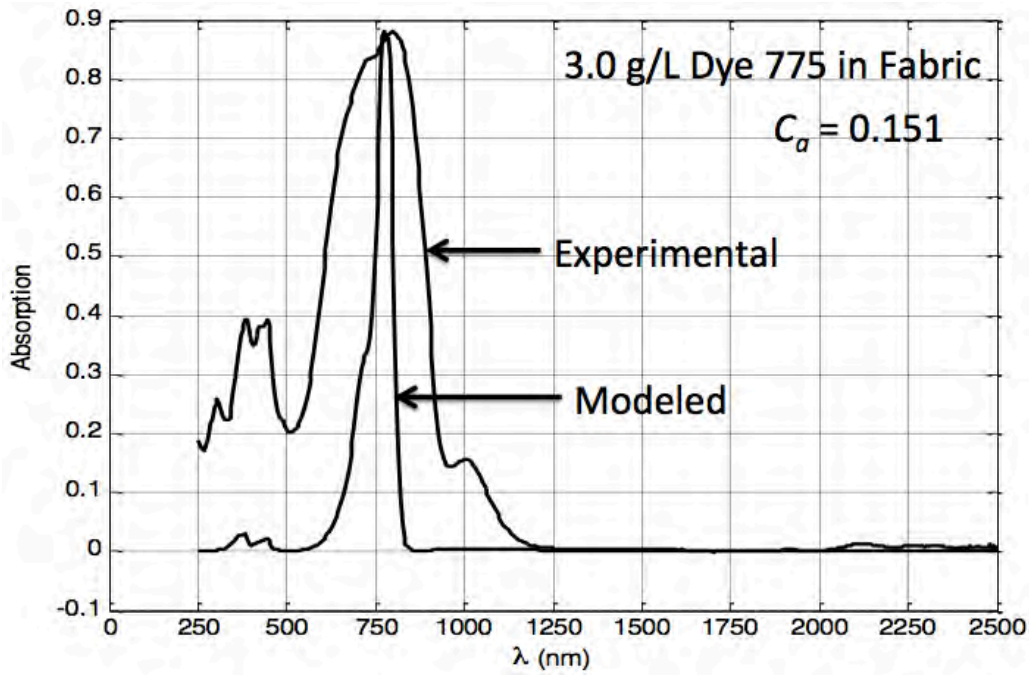


Figure 23e. Comparison of measured and modeled absorption spectra.

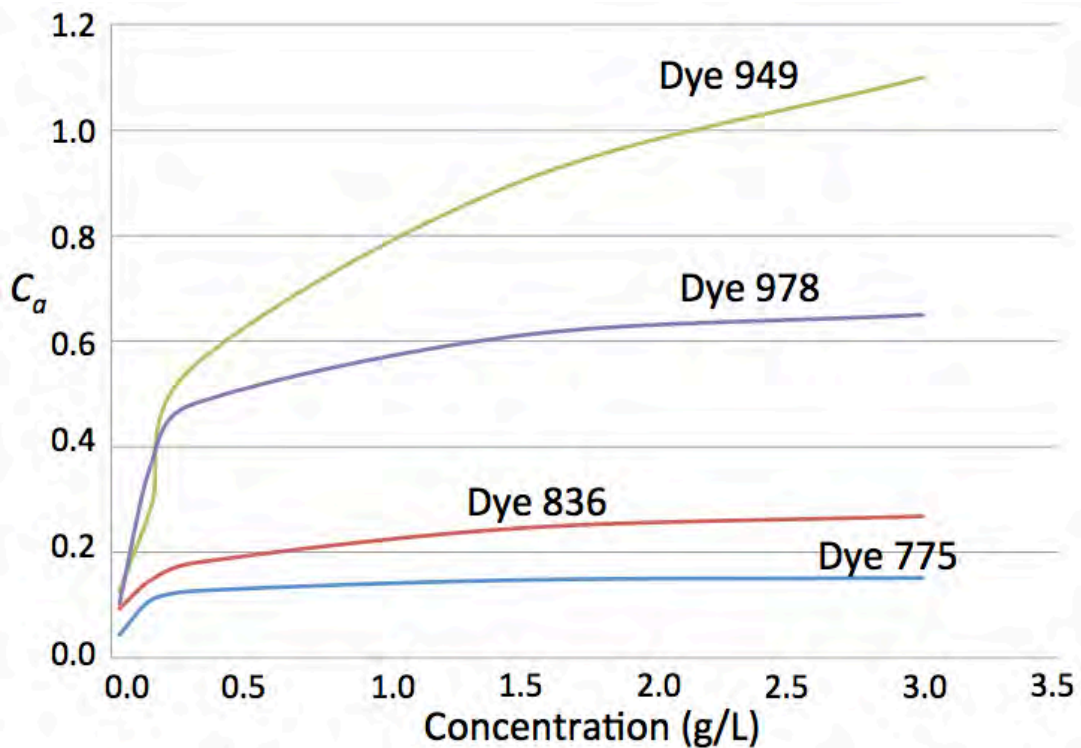


Figure 24. Parameter C_a as a function of dye concentration deposited in fabric for absorption model $C_a \alpha_M(\lambda)$, where $\alpha_M(\lambda)$ has been determined previously by inverse analysis of transmission spectra for dyes in solution.

